01 May 2012

Dissipation Effects in Random Transverse-Field Ising Chains

Jose A. Hoyos

Thomas Vojta
Missouri University of Science and Technology, vojtat@mst.edu

Recommended Citation

J. A. Hoyos and T. Vojta, "Dissipation Effects in Random Transverse-Field Ising Chains," *Physical review B: Condensed matter and materials physics*, vol. 85, no. 17, American Physical Society (APS), May 2012.
The definitive version is available at https://doi.org/10.1103/PhysRevB.85.174403

Dissipation effects in random transverse-field Ising chains

José A. Hoyos[1] and Thomas Vojta[2]
[1]*Instituto de Física de São Carlos, Universidade de São Paulo, C.P. 369, São Carlos, São Paulo 13560-970, Brazil*
[2]*Department of Physics, Missouri University of Science and Technology, Rolla, Missouri 65409, USA*
(Received 10 March 2012; revised manuscript received 19 April 2012; published 2 May 2012)

We study the effects of Ohmic, super-Ohmic, and sub-Ohmic dissipation on the zero-temperature quantum phase transition in the random transverse-field Ising chain by means of an (asymptotically exact) analytical strong-disorder renormalization-group approach. We find that Ohmic damping destabilizes the infinite-randomness critical point and the associated quantum Griffiths singularities of the dissipationless system. The quantum dynamics of large magnetic clusters freezes completely, which destroys the sharp phase transition by smearing. The effects of sub-Ohmic dissipation are similar and also lead to a smeared transition. In contrast, super-Ohmic damping is an irrelevant perturbation; the critical behavior is thus identical to that of the dissipationless system. We discuss the resulting phase diagrams, the behavior of various observables, and the implications to higher dimensions and experiments.

DOI: 10.1103/PhysRevB.85.174403 PACS number(s): 05.10.Cc, 05.70.Fh, 75.10.−b

I. INTRODUCTION

Continuous phase transitions display the remarkable feature of universality: The physics sufficiently close to the transition point is independent of microscopic details; it only depends on a small number of key parameters such as the symmetry of the order parameter, the dimensionality of the system, and the presence or absence of frustration (for reviews see, e.g., Refs. 1 and 2). For this reason, simple prototypical models are extensively used in theoretical studies of continuous phase transitions as their critical behavior can be expected to exactly reproduce that of experimental systems.

Because realistic systems often contain considerable amounts of quenched (time-independent) disorder (randomness), it is important to establish whether or not such disorder is relevant or irrelevant at a continuous phase transition. In other words, is disorder one of the unimportant microscopic details or is it one of the key parameters that determine the critical behavior? Interestingly, the answer to this question is not unique but depends on the transition at hand. Early insight was gained from analyzing the fate of the disorder strength under coarse graining: According to the Harris criterion,[3] disorder is perturbatively relevant at a critical point if its clean correlation length exponent ν fulfills the inequality $d\nu < 2$ with d the space dimensionality. In this case, the critical behavior of the disordered system must differ from that of the clean one. However, the ultimate fate of the transition can not be inferred from the Harris criterion.

In recent years, it has become increasingly clear that rare, strongly interacting spatial regions play an important role in phase transitions in disordered systems. These regions can be (locally) in the ordered phase while the bulk system is still in the disordered phase. Their dynamics becomes very slow because it involves coherently changing the order parameter in a large volume. Griffiths[4,5] showed that these rare regions lead to nonanalyticities in the free energy not just at the critical point, but in an entire parameter region around the transition, which is now known as the Griffiths phase. At generic thermal (classical) transitions, the resulting Griffiths singularities in thermodynamic quantities are very weak and probably unobservable in experiment.[6]

Rare regions are more important for zero-temperature quantum phase transitions, the critical behavior of which is determined by order-parameter fluctuations in space and time. As quenched disorder is perfectly correlated in the time direction, disorder effects are enhanced. The resulting strong quantum Griffiths singularities[7–9] of thermodynamic quantities can take power-law form. The critical point itself remains sharp but can be of exotic infinite-randomness type as was shown by Fisher.[10,11]

At quantum phase transitions, statics and dynamics are intimately coupled. Therefore, changes in the quantum dynamics can cause changes in the thermodynamic behavior. For example, dissipation, i.e., damping of the order-parameter fluctuations due to additional degrees of freedom, can further enhance the rare-region effects. In systems with Ising symmetry, each rare region acts as a two-level system. In the presence of Ohmic dissipation, it undergoes the localization quantum phase transition of the spin-boson problem.[12] Thus, the quantum dynamics of sufficiently large rare regions freezes,[13,14] leading to a smearing of the global phase transition.[15]

In order to gain a more complete understanding of the nonperturbative physics of these dissipative rare regions, the heuristic arguments of Refs. 13–15 need to be complemented by an explicit calculation of a prototypical microscopic model. Schehr and Rieger made significant progress in this direction by applying a numerical strong-disorder renormalization group to the dissipative transverse-field Ising model.[16,17] Their computer simulation results supported the above smeared-transition scenario but focused on the infinite-randomness physics arising at intermediate energies.

In this paper, we derive a comprehensive analytical approach to the quantum phase transition of the transverse-field Ising chain coupled to dissipative baths of harmonic oscillators. The method is a generalization of Fisher's solution[10,11] of the dissipationless case which treats on equal footing the effects of dissipation and disorder. For Ohmic damping, the theory captures the full crossover between the infinite-randomness (and quantum Griffiths) physics at higher energies where the dissipation is less important and the dissipation-dominated smeared transition at low energies. The effects of

sub-Ohmic dissipation are qualitatively similar and also result in a smeared transition. In contrast, super-Ohmic dissipation is irrelevant, and the transition is identical to that of the dissipationless chain. A short account of part of these results was already published in Ref. 18.

Our paper is organized as follows: We define the model in Sec. II. In Secs. III and IV, we derive the renormalization-group recursion relations and the corresponding flow equations. They are solved in Sec. V. Section VI is devoted to phase diagrams, observables, and crossover effects. In Sec. VII, we discuss the applicability of our method for weak disorder, generalizations to higher dimensions, and the relevance of our results for experiments. We conclude and compare with related results in the literature in Sec. VIII.

II. THE HAMILTONIAN

Our model Hamiltonian consists of a one-dimensional random transverse-field Ising model coupled to a bosonic bath[16]

$$H = H_I + H_B + H_C. \tag{1}$$

Here,

$$H_I = -\sum_i J_i \sigma_i^z \sigma_{i+1}^z - \sum_i h_i \sigma_i^x \tag{2}$$

is the Hamiltonian of the (dissipationless) random transverse-field Ising chain. The spin-1/2 degree of freedom at site i is described by the Pauli matrices $\boldsymbol{\sigma}_i$, the local ferromagnetic interaction is represented by J_i, and the local transverse field h_i controls the strength of the quantum fluctuations.

Dissipation, i.e., damping of the quantum fluctuations, is introduced by coupling the z component of each spin to an independent bath of quantum harmonic oscillators.[19] The bath Hamiltonian reads as

$$H_B = \sum_{k,i} \omega_{k,i} \left(a_{k,i}^\dagger a_{k,i} + \frac{1}{2} \right), \tag{3}$$

with $\omega_{k,i}$ being the frequency of the kth harmonic oscillator coupled to the spin at site i, and $a_{k,i}$ ($a_{k,i}^\dagger$) being the usual annihilation (creation) operators. (Note that we set $\hbar = 1$.) Finally, the coupling between the spins and their respective baths is given by

$$H_C = \sum_i \sigma_i^z \sum_k \lambda_{k,i} (a_{k,i}^\dagger + a_{k,i}), \tag{4}$$

with $\lambda_{k,i}$ being the strength of the interaction.

All relevant information about the bosonic baths is encoded in their spectral densities $\mathcal{E}_i$, which can be parametrized as

$$\mathcal{E}_i(\omega) = \pi \sum_k \lambda_{k,i}^2 \delta(\omega - \omega_{k,i}) = \frac{\pi}{2} \alpha_i \omega_{0,i}^{1-s} \omega^s \quad (\omega < \omega_{c,i}). \tag{5}$$

Here, $\omega_{c,i}$ is an ultraviolet cutoff energy, and α_i is a dimensionless measure of the dissipation strength. The microscopic energy scale $\omega_{0,i}$ is often identified with the cutoff $\omega_{c,i}$. However, we need to keep the two energies separate because the cutoff $\omega_{c,i}$ will flow within our renormalization-group procedure, while $\omega_{0,i}$ (the bare cutoff energy) will not. Depending on the value of the exponent s, different types of dissipation can be distinguished. $s = 1$ corresponds to the experimentally important Ohmic case. For $s > 1$, the bath is super-Ohmic, which leads to qualitatively weaker dissipation effects as there are fewer bath states at low energies. For $s < 1$, the bath is dubbed sub-Ohmic.

We emphasize that in the model (1), each spin is coupled to its own (local) oscillator bath. Therefore, these baths damp the local order-parameter fluctuations, i.e., they induce a long-range interaction in time. However, they do not produce interactions between different sites. If we coupled all spins to the same (global) oscillator bath, we would also obtain an effective interaction, mediated by the bath oscillators, between the spins at different sites. This interaction would be analogous to the Ruderman-Kittel-Kasuya-Yosida (RKKY) interaction between localized magnetic moments in metals.

Quenched disorder is implemented by taking all parameters in the Hamiltonian (1), i.e., the interactions J_i, the transverse fields h_i, the dissipation strengths α_i, as well as the bath energy scales $\omega_{c,i}$ and $\omega_{0,i}$ to be independent random variables. Actually, making one of these quantities random is sufficient because, under the renormalization-group flow (discussed in Secs. III and IV), the other quantities acquire randomness even if their bare values are not random. In the following, we thus assume that in the bare system only J_i and h_i are random, with probability distributions $P_I(J)$ and $R_I(h)$, while $\alpha_i = \alpha_I \equiv \alpha$, $\omega_{0,i} = \omega_I$, and $\omega_{c,i} = \omega_c$ are uniform. We also restrict ourselves to the experimentally most interesting case[12] of the bath energy ω_I being the largest energy scale in the problem $\omega_I \gg h_i, J_i$.

III. RENORMALIZATION-GROUP RECURSION RELATIONS

We now turn to the derivation of our theory. Our intent is to apply a real-space-based strong-disorder renormalization-group method to the Hamiltonian (1). This technique was introduced to tackle random antiferromagnetic spin-1/2 chains[20,21] and has been successfully generalized to many disordered systems (for a review, see Ref. 22). Its philosophy is to successively integrate out the degrees of freedom with the highest local energies. This approach is justified *a posteriori* if the renormalized disorder strength becomes very large.

A. Review of the dissipationless case

The strong-disorder renormalization group of the dissipationless random transverse-field Ising chain (2) was derived and solved by Fisher.[10,11] One starts by identifying the highest local energy scale, $\Omega = \max\{h_i, J_i\}$, in the system.

If the largest energy is an interaction, say, J_2, the low-energy states are those in which σ_2^z and σ_3^z are parallel: $|++\rangle$ and $|--\rangle$. Therefore, the cluster of sites 2 and 3 can be recast as a single effective spin-1/2 degree of freedom, the effective magnetic moment of which is $\tilde{\mu} = \mu_2 + \mu_3$. The transverse fields h_2 and h_3 will lift the degeneracy between $|++\rangle$ and $|--\rangle$ in second order of perturbation theory, yielding an effective transverse field $\tilde{h} = h_2 h_3 / J_2$ for the new spin.

In contrast, when the largest energy is a transverse field, say h_2, the spin at site 2 is rapidly fluctuating between the

$|+\rangle$ and $|-\rangle$ eigenstates (in z direction). It hence does not contribute to magnetization and can be decimated from the chain. The neighboring spins σ_1 and σ_3 become connected via an effective coupling $\tilde{J} = J_1 J_2/h_2$, also obtained in second order of perturbation theory.

This summarizes the renormalization-group recursion relations for the dissipationless case. Note that the recursion relations are symmetric under exchanging h and J, reflecting the self-duality of the Hamiltonian (2).

B. Generalization to the dissipative case

The generalization of the strong-disorder renormalization group to the full Hamiltonian (1) is not unique because the bosonic baths can be incorporated in different ways. One possibility is implemented in the numerical work of Refs. 16 and 17. Here, the renormalization-group step still consists of identifying the largest of all the interactions and transverse fields, $\Omega = \max\{J_i, h_i\}$. Before decimating the corresponding high-energy degree of freedom, one integrates out the high-energy bath oscillators of the involved sites. This modifies the transverse fields and thus changes the recursion relations. Furthermore, the bath cutoff ω_c becomes site dependent. While this scheme appears to work very well numerically, we found it hard to implement analytically as it yields nonanalytic flow equations for the distributions of J, h, and μ.

This difficulty is overcome by integrating out the oscillator degrees of freedom together with the lattice modes (related to strong interactions and transverse fields). We thus define the renormalization-group energy scale as $\Omega = \max\{J_i, h_i, \omega_c/p\}$, where $p \gg 1$ is a dimensionless constant, the importance of which will become clear below in the context of adiabatic renormalization. A renormalization-group step now consists of decimating either an interaction $J_i = \Omega$, a transverse field $h_i = \Omega$, or an oscillator with frequency $\omega_{k,i} = p\Omega$. Upon lowering the renormalization-group energy scale from Ω to $\Omega - d\Omega$, the bath cutoff ω_c is thus reduced by $p\, d\Omega$ at *all* sites. In this sense, the renormalization of the baths is *global*, and not local as in the scheme of Refs. 16 and 17. This allows us to treat ω_c as a nonrandom variable.

As it turns out, this modified scheme is analytically tractable. In the following sections, we derive the resulting recursion relations.

C. Adiabatic renormalization of the bosonic baths

In order to understand the effects of dissipation on the quantum fluctuations, we first consider a single spin coupled to a bosonic bath, i.e., the well-known spin-boson problem[12] given by

$$H_{\rm sb} = -h\sigma^x + \sigma^z \sum_k \lambda_k (a_k^\dagger + a_k) + \sum_k \omega_k \left(a_k^\dagger a_k + \frac{1}{2} \right). \tag{6}$$

The idea of the adiabatic renormalization is to eliminate high-frequency oscillators in a Born-Oppenheimer type of approximation. Let us assume that all oscillators of frequencies greater than ph with $p \gg 1$ can instantaneously follow the spin. We now wish to integrate out these fast oscillators. To this end, consider the Hamiltonian

$$\begin{aligned} H_0 &= \sigma^z \sum_{\omega_k > ph} \lambda_k (a_k^\dagger + a_k) + \sum_{\omega_k > ph} \omega_k \left(a_k^\dagger a_k + \frac{1}{2} \right) \\ &= \sum_{\omega_k > ph} \omega_k \left(b_k^\dagger b_k + \frac{1}{2} \right), \end{aligned} \tag{7}$$

with $b_k = a_k + (\lambda_k/\omega_k)\sigma^z$. Here, the sums are over the fast oscillators only, and an unimportant constant has been dropped. Notice that the difference between a_k and b_k simply represents a shift of the oscillator's rest position of magnitude $x_{0k} = -\sigma^z \lambda_k \sqrt{2/(m_k \omega_k^3)}$. (Recall that $x_k \sqrt{2 m_k \omega_k} \equiv a_k^\dagger + a_k$, with m_k being the mass of the kth oscillator.) Using the translation operator, the shifted ground state of oscillator k can be represented as

$$|0_{k,\sigma^z}\rangle = e^{i x_{0k} p_k} |0_k\rangle \equiv \exp\left[\sigma^z \frac{\lambda_k}{\omega_k} (a_k^\dagger - a_k) \right] |0_k\rangle, \tag{8}$$

where $|0_k\rangle$ denotes the ground state of the unperturbed oscillator. Finally, the ground state of H_0 is doubly degenerate with eigenvectors

$$|\Psi_\pm\rangle = \frac{1}{\sqrt{2}} \left(|+\rangle \prod_{\omega_k > ph} |0_{k,+}\rangle \pm |-\rangle \prod_{\omega_k > ph} |0_{k,-}\rangle \right). \tag{9}$$

The transverse-field term in the Hamiltonian $H_1 = -h\sigma^x$ lifts this degeneracy. The tunnel splitting, i.e., the tunneling rate of the spin σ between $|+\rangle$ and $|-\rangle$, is given by the energy difference $E_+ - E_- = 2h' = \langle \Psi_+ | H_1 | \Psi_+ \rangle - \langle \Psi_- | H_1 | \Psi_- \rangle = 2h \prod_{\omega_k > ph} \langle 0_{k,+} | 0_{k,-} \rangle$. Therefore, we can replace the spin coupled to the fast oscillators by an effective free spin with a renormalized transverse field

$$\begin{aligned} h' &= h \prod_{\omega_k > ph} \langle 0_{k,+} | 0_{k,-} \rangle = h \exp\left[-2 \sum_{\omega_k > ph} \left(\lambda_k^2 / \omega_k^2 \right) \right] \\ &= h \exp\left[-\frac{2}{\pi} \int_{ph}^{\omega_c} \frac{\mathcal{E}(\omega)}{\omega^2} d\omega \right], \end{aligned} \tag{10}$$

which depends exponentially on the spectral density (5). Now, as long as h' remains below the cutoff energy $\omega_c' = ph$ of the remaining oscillators, this procedure can be iterated until convergence.

The qualitative features of this adiabatic renormalization procedure depend on the character of the dissipation.[12] For super-Ohmic dissipation ($s > 1$), h' always converges to a finite value $h^* > 0$, regardless of the dissipation strength α. Thus, the spin effectively *decouples* from the bath and remains tunneling in the presence of dissipation. In contrast, h^* vanishes for sub-Ohmic dissipation ($0 < s < 1$), implying that the damping localizes the spin (at least in the limit of small h). In the Ohmic case, the behavior depends on the dissipation strength α. As long as $\alpha < 1$, the transverse field converges to a nonzero value $h^* = h(ph/\omega_c)^{\alpha/(1-\alpha)}$, while it converges to $h^* = 0$ for $\alpha > 1$. Based on the heuristic arguments of Ref. 15, we therefore expect a smeared quantum phase transition in the sub-Ohmic and Ohmic cases.

Let us now use the adiabatic renormalization of the oscillators within the strong-disorder renormalization-group

scheme of the full dissipative random transverse-field Ising chain (1), as outlined in Sec. III B. Our intent is to lower the renormalization-group energy scale from Ω to $\Omega - d\Omega$. To do so, we need to integrate out all oscillators in the frequency range between $p(\Omega - d\Omega)$ and $p\Omega$. Because the interaction terms in Eq. (1) are diagonal in the σ^z basis, they can simply be incorporated in H_0. Thus, when integrating out the high-frequency oscillators in all baths, the transverse fields renormalize according to

$$h_i' = h_i \exp\left[-\alpha_i \omega_I^{1-s} \int_{p\Omega - p\,d\Omega}^{p\Omega} d\omega\, \omega^{s-2} \right] = h_i \left[1 - \alpha_i \left(\frac{\Omega}{\Omega_I} \right)^{s-1} \frac{d\Omega}{\Omega} \right]. \quad (11)$$

Here, we have used the relation $\omega_I = p\Omega_I$ between the bare renormalization-group energy scale Ω_I and the bare oscillator cutoff frequency ω_I. Notice that the renormalized fields h_i' do not depend on the arbitrary constant $p \gg 1$.

Equation (11) reveals a crucial difference between the super-Ohmic, Ohmic, and sub-Ohmic cases. In the super-Ohmic case, the term renormalizing the transverse field is suppressed by a factor $(\Omega/\Omega_I)^{s-1}$, which vanishes as the energy scale Ω goes to zero. This suggests that super-Ohmic dissipation becomes unimportant at sufficiently low-energy scales. Our calculations in the following will show that this is indeed the case. In contrast, the term renormalizing the transverse field remains finite or even diverges with $\Omega \to 0$ in the Ohmic and sub-Ohmic cases, respectively.

D. Decimating a site

Let us now focus on integrating out a site, say site 2, because its transverse field h_2 is at the renormalization-group energy scale Ω. It is important to realize that if $h_2 = \Omega$, the field actually has reached its fully converged value h_2^* with respect to the adiabatic renormalization discussed in the last section (because all remaining oscillators have frequencies below ph_2). Hence, the spin σ_2 has decoupled from its bath, and decimation of the site proceeds as in the undamped case.[11] We consider $H_0 = -h_2\sigma_2^x$ as the unperturbed Hamiltonian, while the interactions of σ_2 with its neighbors are treated perturbatively: $H_1 = -(J_1\sigma_1^z + J_2\sigma_3^z)\sigma_2^z$. In second order of perturbation theory, the low-lying spectrum of the cluster of sites 1, 2, and 3 can be represented by $H_{\rm eff} = -\tilde{J}\sigma_1^z\sigma_3^z$ with

$$\tilde{J} = \frac{J_1 J_2}{h_2}. \quad (12)$$

This means that the strongly fluctuating spin σ_2 is removed from the chain, while the neighboring spins are coupled via a renormalized weaker bond $\tilde{J}$.

E. Decimating an interaction

Finally, the last possible decimation happens when an interaction, say J_2, is at the renormalization-group energy scale Ω. In this case, we consider the cluster of sites 2 and 3 as well as its coupling to the neighboring sites 1 and 4. The unperturbed part of the Hamiltonian reads as $H_0 = -J_2\sigma_2^z\sigma_3^z$, while $H_{1x} = -h_2\sigma_2^x - h_3\sigma_3^x$ and $H_{1z} = -J_1\sigma_1^z\sigma_2^z - J_3\sigma_3^z\sigma_4^z$ as well as $H_{1\rm diss} = \sum_{i=2}^3 \sigma_i^z \sum_k [\lambda_{k,i}(a_{k,i}^\dagger + a_{k,i}) + \omega_{k,i}(a_{k,i}^\dagger a_{k,i} + 1/2)]$ are treated as perturbations. As in the undamped case, the low-energy states are those in which σ_2^z and σ_3^z are parallel. Therefore, the cluster of sites 2 and 3 can be replaced by a single effective spin $\tilde{\sigma}$, the states $|+\rangle$ and $|-\rangle$ of which represent $|\sigma_2\sigma_3\rangle = |++\rangle$ and $|\sigma_2\sigma_3\rangle = |--\rangle$, respectively. Treating the perturbations to lowest nonvanishing order (first order of perturbation theory for H_{1z} and $H_{1\,\rm diss}$ but second order for H_{1x}), yields the effective Hamiltonian

$$H_{\rm eff} = -J_1\sigma_1^z\tilde{\sigma}^z - J_3\tilde{\sigma}^z\sigma_4^z - \tilde{h}\tilde{\sigma}^x + \tilde{\sigma}^z \sum_k \tilde{\lambda}_k(a_k^\dagger + a_k) + \omega_k\left(a_k^\dagger a_k + \frac{1}{2}\right). \quad (13)$$

The renormalized transverse field $\tilde{h}$ is smaller than either of the original ones and given by

$$\tilde{h} = \frac{h_2 h_3}{J_2}. \quad (14)$$

The magnetic moment associated with the renormalized spin $\tilde{\sigma}$ is the sum of the moments of σ_2^z and σ_3^z,

$$\tilde{\mu} = \mu_2 + \mu_3, \quad (15)$$

while the dissipative bath coupled to $\tilde{\sigma}$ has spectral density

$$\tilde{\mathcal{E}}(\omega) = \frac{\pi}{2}\tilde{\alpha}\omega_I^{1-s}\omega^s \quad \text{with} \quad \tilde{\alpha} = \alpha_2 + \alpha_3. \quad (16)$$

This means the renormalized dissipation strength of a cluster increases with its magnetic moment. We can thus parametrize the local dissipation strength α_i in terms of the magnetic moment μ_i as

$$\alpha_i = \alpha\mu_i. \quad (17)$$

This has the advantage that we do not have to separately keep track of the probability distribution of the dissipation strengths during the renormalization-group flow.

We note in passing that one can also include $H_{1\,\rm diss}$ in the unperturbed Hamiltonian, as was done in Ref. 17. This leads to more complicated algebra but results in the same recursions (13)–(16) at the approximation level considered here.

F. Summary of the decimation procedure

The entire decimation procedure resulting from the steps outlined in Secs. III C to III E can be summarized as follows (see Fig. 1 for a schematic illustration).

In lowering the renormalization-group energy scale from Ω to $\Omega - d\Omega$, we first integrate out all oscillators with frequencies in the range $[p\Omega - p\,d\Omega, p\Omega]$ in adiabatic renormalization. This modifies *all* transverse fields according to Eq. (11) [see Fig. 1(a)].

After this global decimation, we integrate out all transverse fields and interactions in the energy range $[\Omega - d\Omega, \Omega]$. (As these decimations are local, they do not interfere with each other.) In the case of decimating a transverse field, the corresponding site and bath are removed from the system, yielding an effective coupling between the neighboring spins given by Eq. (12) [see Fig. 1(b.i)]. When integrating out an interaction, the corresponding spins are replaced by a single effective one. The transverse field acting on this spin and its effective magnetic moment are given by Eqs. (14) and (15). The spectral function of the bosonic bath coupling to the

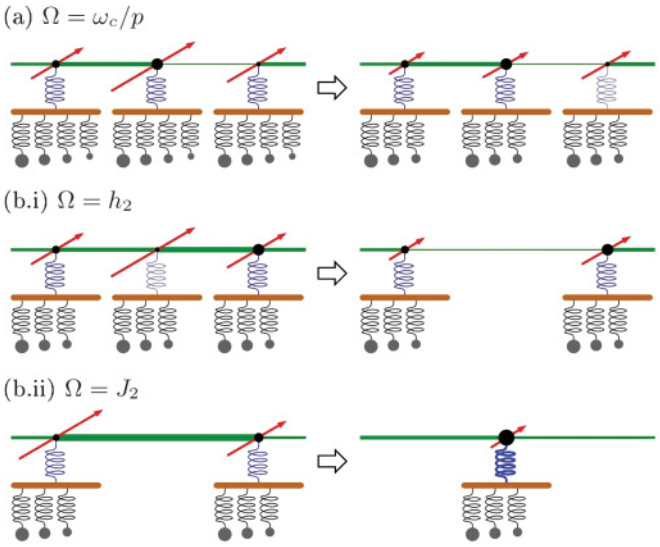

FIG. 1. (Color online) Decimation scheme. The magnitudes of the transverse fields, interactions, and magnetic moments are depicted by the length of the arrows, the thickness of the lines, and the size of the dots, respectively. The bosonic baths are depicted by the array of springs and oscillators in which lighter (small) oscillators are faster. Finally, the magnitude of the coupling to the bath (or the local dissipation strength) is depicted by the thickness of the spring connecting the spin to the bath. (a) *Global* adiabatic renormalization of the fast oscillators, (b.i) decimation of a strong *local* transverse field, and (b.ii) decimation of a strong *local* interaction.

effective spin has the same exponent s as the original baths, but the dissipation strengths increases according to Eq. (16) [see Fig. 1(b.ii)]. This last renormalization is taken into account automatically if one defines the local α_i as in Eq. (17).

IV. FLOW EQUATIONS

The strong-disorder renormalization group consists in iterating the decimation steps of Sec. III, and so reducing the renormalization-group energy scale $\Omega = \max\{J_i, h_i, \omega_c/p\}$ to zero. In this process, the probability distributions of the interactions, transverse fields, and magnetic moments change. In this section, we derive the renormalization-group flow equations for these distributions. In contrast to the dissipationless case, where the magnetic moment does not enter the recursions for the transverse fields and interactions,[10,11] our recursion relation (11) couples the magnetic moments μ and transverse fields h (via $\alpha_i = \mu_i \alpha$). In addition to the distribution $P(J;\Omega)$ of the interactions, we therefore need to consider the *joint* distribution of transverse fields and magnetic moments $R(h,\mu;\Omega)$. The last argument of these distributions makes explicit the dependence on the renormalization-group energy scale Ω. Occasionally, we will also use the reduced distribution of the transverse fields $R_h(h;\Omega) = \int_0^\infty R(h,\mu;\Omega)d\mu$.

A. Flow of $P(J;\Omega)$

The distribution of the interactions J only changes when a site (a strong transverse field) is decimated. Upon reducing the energy scale from Ω to $\Omega - d\Omega$, $P(J;\Omega)$ thus transforms almost as in the undamped case:[11]

$$P(J;\Omega - d\Omega)\{1 - d\Omega[P(\Omega;\Omega) + R'_{h'}(\Omega;\Omega)]\} = P(J;\Omega) - d\Omega\, R'_{h'}(\Omega;\Omega)\int dJ_1 dJ_2 P(J_1;\Omega)P(J_2;\Omega) \times \left[\delta(J - J_1) + \delta(J - J_2) - \delta\left(J - \frac{J_1 J_2}{\Omega}\right)\right], \quad (18)$$

where $R'_{h'}(h';\Omega)$ is the distribution of transverse fields *after* integrating out the fast bath oscillators in the energy interval $[p\Omega - p\,d\Omega, p\Omega]$ according to Eq. (11). The term between the brackets on the left-hand side of Eq. (18) guarantees the normalization of $P(J;\Omega - d\Omega)$ (decimating either a site or an interaction each reduces the number of interactions in the system by one). The second term on the right-hand side implements the decimation of a site (transverse field), which happens with probability $d\Omega\, R'_{h'}(\Omega;\Omega)$. The first and second delta functions in this term remove the neighboring couplings, while the third one inserts the renormalized one, as given by Eq. (12). The integral over J_1 and J_2, weighted by $P(J_1;\Omega)P(J_2;\Omega)$, sums over all possible values of neighboring couplings.

The only difference to the undamped case stems from the fact that the decimation of a site is determined by the distribution $R'_{h'}(h';\Omega)$ of the transverse fields *after* integrating out the fast bath oscillators rather than the distribution of the unrenormalized fields $R_h(h;\Omega)$. Using (11), the probability $R'_{h'}(\Omega;\Omega)d\Omega$ of having a decimation of a site can be found as

$$\begin{aligned} R'_{h'}(\Omega;\Omega)d\Omega &= \int_0^\infty d\mu \int_{\Omega - d\Omega}^{\Omega} dh' R'(h',\mu;\Omega) \\ &= \int_0^\infty d\mu \int_{\Omega - d\Omega + \alpha\mu(\Omega/\Omega_I)^{s-1}d\Omega}^{\Omega} dh\, R(h,\mu;\Omega) \\ &= [1 - \alpha\overline{\mu}_\Omega(\Omega/\Omega_I)^{s-1}]R_h(\Omega;\Omega)d\Omega, \end{aligned} \quad (19)$$

where $\overline{\mu}_\Omega = \int_0^\infty \mu R(\Omega,\mu;\Omega)d\mu / \int_0^\infty R(\Omega,\mu;\Omega)d\mu$ is the mean magnetic moment to be decimated at the energy scale Ω. Equation (19) can be understood as follows (see Fig. 2 for an illustration). Before integrating out the fast oscillators, the potential fields to be decimated are those in the range $[\Omega - d\Omega, \Omega]$ highlighted in Fig. 2(a). However, after eliminating these oscillators, some of those fields are

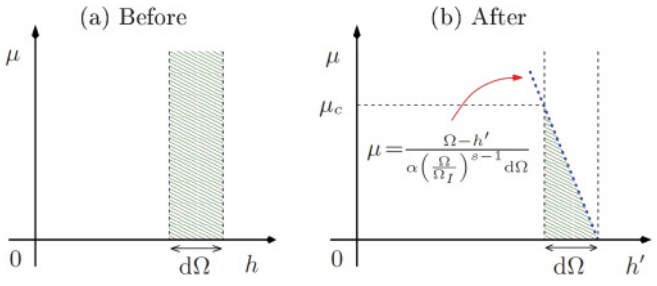

FIG. 2. (Color online) Schematic of the possible transverse-field decimations in the h vs μ plane. (a) Before the integration of the fast oscillators, the hatched area represents all the potential fields to be decimated. (b) After integrating out the oscillators, some of these fields have been shifted below $\Omega - d\Omega$ and are not eligible to be decimated anymore, only those in the triangular shaded area still are. The dashed line $h = \Omega$ maps into the dotted line $\mu = (\Omega - h')/[\alpha(\Omega/\Omega_I)^{s-1}d\Omega]$ after the adiabatic-renormalization step (11).

renormalized downward out of decimating region. Only the fields in the hatched area of Fig. 2(b) may still be decimated.

Equation (19) implies that any cluster with magnetic moment larger than $\mu_c(\Omega) = 1/[\alpha(\Omega/\Omega_I)^{s-1}]$ will never be decimated. For Ohmic dissipation $s = 1$, this means that there is an energy-independent cutoff cluster size $\mu_c = 1/\alpha$ (and thus a finite length scale). All clusters with $\mu > \mu_c$ will become frozen as their transverse fields h iterate to zero with $\Omega \to 0$. This will lead to the smearing of the quantum phase transition. In contrast, for super-Ohmic dissipation $s > 1$, the cutoff cluster size $\mu_c(\Omega)$ diverges with $\Omega \to 0$, which reflects the fact that super-Ohmic dissipation can not prevent the tunneling of even the largest clusters.

B. Flow of $R(h,\mu;\Omega)$

The joint distribution $R(h,\mu;\Omega)$ of transverse fields and magnetic moments changes when an interaction is decimated. It also changes in response to the adiabatic renormalization of the fast oscillators. As a result, the flow equation of $R(h,\mu;\Omega)$ is more complicated than in the dissipationless case:[11]

$$\begin{aligned} &R(h,\mu;\Omega - d\Omega)\{1 - d\Omega[P(\Omega;\Omega) + R'_{h'}(\Omega;\Omega)]\} \\ &\quad = R(h,\mu;\Omega) - d\Omega\, P(\Omega;\Omega) \int dh_2 d\mu_2 dh_3 d\mu_3 R(h_2,\mu_{2;\Omega}) R(h_3,\mu_3;\Omega) \\ &\qquad \times \left[\delta(h-h_2)\delta(\mu-\mu_2) + \delta(h-h_3)\delta(\mu-\mu_3) - \delta\left(h - \frac{h_2 h_3}{\Omega}\right)\delta(\mu-\mu_2-\mu_3)\right] \\ &\qquad - \int dh_2 d\mu_2 R(h_2,\mu_2;\Omega)[\delta(h-h_2)\delta(\mu-\mu_2) - \delta(h-h'_2)\delta(\mu-\mu_2)], \end{aligned} \tag{20}$$

where h'_2 is given by Eq. (11). The second term on the right-hand side of Eq. (20) implements the change in the fields and magnetic moments when an interaction is decimated. The third term implements the adiabatic renormalization due the decimation of the fast bath oscillators. The normalization term [between the brackets on the left-hand side of Eq. (20)] takes the same form as in Eq. (18) because decimating either a site or an interaction each reduces the number of sites (i.e., transverse fields) in the system by one.

After some tedious but straightforward algebra, Eqs. (18) and (20) simplify to

$$\begin{aligned} -\frac{\partial}{\partial\Omega}P(J;\Omega) &= \left\{P(\Omega;\Omega) - \left[1 - \alpha\overline{\mu}_\Omega\left(\frac{\Omega}{\Omega_I}\right)^{s-1}\right]R_h(\Omega;\Omega)\right\}P(J;\Omega) \\ &\quad + \left[1 - \alpha\overline{\mu}_\Omega\left(\frac{\Omega}{\Omega_I}\right)^{s-1}\right]R_h(\Omega;\Omega)\int dJ_1 dJ_2 P(J_1;\Omega)P(J_2;\Omega)\delta\left(J - \frac{J_1 J_2}{\Omega}\right), \end{aligned} \tag{21}$$

$$\begin{aligned} -\frac{\partial}{\partial\Omega}R(h,\mu;\Omega) &= \left\{\left[1 - \alpha\overline{\mu}_\Omega\left(\frac{\Omega}{\Omega_I}\right)^{s-1}\right]R_h(\Omega;\Omega) - P(\Omega;\Omega)\right\}R(h,\mu;\Omega) + \frac{\alpha\mu}{\Omega}\left(\frac{\Omega}{\Omega_I}\right)^{s-1}\left(1 + h\frac{\partial}{\partial h}\right)R(h,\mu;\Omega) \\ &\quad + P(\Omega;\Omega)\int dh_2 d\mu_2 dh_3 d\mu_3 R(h_2,\mu_2;\Omega)R(h_3,\mu_3;\Omega)\delta\left(h - \frac{h_2 h_3}{\Omega}\right)\delta(\mu-\mu_2-\mu_3). \end{aligned} \tag{22}$$

All terms proportional to α are due to dissipation. Those multiplying $\overline{\mu}_\Omega$ correspond to a reduced probability of decimating a site because the transverse fields are renormalized downward by the dissipative baths. The additional term (the second one on the right-hand side) in Eq. (22) corresponds to the global change of all transverse fields when the oscillators are integrated out. The flow equations of the undamped case[10,11] are recovered as expected if we set $\alpha = 0$.

Moreover, in the undamped case, the magnetic moments in Eq. (22) can be integrated out, resulting in flow equations for the reduced distribution $R_h(h;\Omega)$ of the transverse fields. This is no longer the case for $\alpha \neq 0$, and the fixed-point distributions for fields and magnetic moments have to be obtained jointly.

V. FORMAL SOLUTION OF THE FLOW EQUATIONS

In this section, we solve the renormalization-group flow equations (21) and (22). To this end, we first change to logarithmic energy variables. We then perform a general rescaling transformation, which allows us to identify fixed-point distributions of the flow equations.

A. Logarithmic variables

We introduce a logarithmic measure of the renormalization-group energy scale

$$\Gamma = \ln(\Omega_I/\Omega) \tag{23}$$

as well as the logarithmic variables

$$\zeta = \ln(\Omega/J) \quad \text{and} \quad \beta = \ln(\Omega/h), \tag{24}$$

describing the interactions and transverse fields, respectively.[10,11] This is advantageous because the multiplicative recursion relations (12) and (14) turn into additive ones: $\tilde{\zeta} = \zeta_1 + \zeta_2$ and $\tilde{\beta} = \beta_2 + \beta_3$.

The probability distributions π and ρ of the logarithmic variables can be defined as $\pi(\zeta;\Gamma)d\zeta = P(J;\Omega)dJ$, $\rho(\beta,\mu;\Gamma)d\beta\, d\mu = R(h,\mu;\Omega)dh\, d\mu$. Rewriting the flow equations (21) and (22) in terms of these distributions yields

$$\frac{\partial\pi}{\partial\Gamma} = \frac{\partial\pi}{\partial\zeta} + [\pi_0 - (1-\alpha\overline{\mu}_0 e^{-(s-1)\Gamma})\rho_{\beta,0}]\pi(\zeta) + (1-\alpha\overline{\mu}_0 e^{-(s-1)\Gamma})\rho_{\beta,0}\pi \overset{\zeta}{\otimes} \pi, \tag{25}$$

$$\frac{\partial\rho}{\partial\Gamma} = \frac{\partial\rho}{\partial\beta} + [(1-\alpha\overline{\mu}_0 e^{-(s-1)\Gamma})\rho_{\beta,0} - \pi_0]\rho(\beta,\mu) - \alpha\mu e^{-(s-1)\Gamma}\frac{\partial\rho}{\partial\beta} + \pi_0\rho \overset{\beta,\mu}{\otimes} \rho, \tag{26}$$

where $\overline{\mu}_0 \equiv \overline{\mu}_{\beta=0} = \overline{\mu}_\Omega$ is the mean magnetic moment to be decimated. $\pi_0 = \pi(0;\Gamma)$ determines the probability of decimating an interaction while $\rho_{\beta,0} = \int \rho(0,\mu;\Gamma)d\mu$ determines the probability for decimating a transverse field. The symbol $\otimes$ denotes the convolution $\pi \overset{\zeta}{\otimes} \pi = \int d\zeta_1 d\zeta_2 \pi(\zeta_1)\pi(\zeta_2)\delta(\zeta - \zeta_1 - \zeta_2)$.

The origin of each term in Eqs. (25) and (26) can be easily tracked. The first term on the right-hand side of each equation is due to the change of the variable ζ or β when Γ changes. The second terms ensure the normalizations of the distributions. The last ones are responsible for implementing the recursion relations (12) and (14), and the third term in Eq. (26) implements the damping of the transverse fields according to Eq. (11).

B. Rescaling

We now look for fixed-point solutions of the flow equations (25) and (26), i.e., for distributions π and ρ that are stationary under the renormalization-group flow. From the solution of the dissipationless case,[10,11] it is known that such fixed points only emerge after the variables ζ and β are appropriately rescaled. Let us consider the general transformations $\eta = \zeta/f_\zeta(\Gamma)$, $\theta = \beta/f_\beta(\Gamma)$, and $\nu = \mu/f_\mu(\Gamma)$, where the scale factors $f_{\zeta,\beta,\mu}(\Gamma)$ are functions of the logarithmic energy cutoff Γ only. Transforming the flow equations to the distributions $\mathcal{P}(\eta)$ and $\mathcal{R}(\theta,\nu)$ of the rescaled variables yields

$$\frac{\partial\mathcal{P}}{\partial\Gamma} = \frac{\dot{f}_\zeta}{f_\zeta}\left(\mathcal{P} + \eta\frac{\partial\mathcal{P}}{\partial\eta}\right) + \frac{1}{f_\zeta}\left(\frac{\partial\mathcal{P}}{\partial\eta} + \mathcal{P}_0\mathcal{P}\right) + \frac{1}{f_\beta}(1-\alpha\overline{\nu}_0 f_\mu e^{-(s-1)\Gamma})\mathcal{R}_{\theta,0}(\mathcal{P} \overset{\eta}{\otimes} \mathcal{P} - \mathcal{P}), \tag{27}$$

$$\frac{\partial\mathcal{R}}{\partial\Gamma} = \frac{\dot{f}_\beta}{f_\beta}\left(\mathcal{R} + \theta\frac{\partial\mathcal{R}}{\partial\theta}\right) + \frac{\dot{f}_\mu}{f_\mu}\left(\mathcal{R} + \nu\frac{\partial\mathcal{R}}{\partial\nu}\right) + \frac{1}{f_\beta}\left[\frac{\partial\mathcal{R}}{\partial\theta} + (1-\alpha\overline{\nu}_0 f_\mu e^{-(s-1)\Gamma})\mathcal{R}_{\theta,0}\mathcal{R}\right] - \alpha\nu\frac{f_\mu}{f_\beta}e^{-(s-1)\Gamma}\frac{\partial\mathcal{R}}{\partial\theta} + \frac{1}{f_\zeta}\mathcal{P}_0(\mathcal{R} \overset{\theta,\nu}{\otimes} \mathcal{R} - \mathcal{R}), \tag{28}$$

where $\dot{f} = df/d\Gamma$, $\overline{\nu}_0 \equiv \overline{\nu}_{\theta=0}$, $\mathcal{P}_0 = \mathcal{P}(0;\Gamma)$, and $\mathcal{R}_{\theta,0} = \int \mathcal{R}(0,\nu;\Gamma)d\nu$.

C. Fixed-point distributions

The low-energy solutions of the flow equations describe stable phases or critical points. Before analyzing the equations in detail, we can already identify two simple solutions that correspond to the conventional paramagnetic and ferromagnetic phases. The key feature is a separation of scales between the interactions and the transverse fields.

When all interactions J are larger than all transverse fields h (i.e., their distributions do not overlap), the renormalization-group procedure will only decimate interactions until every site is included in the infinite cluster formed. This happens at a finite energy scale, viz., the minimum value of J in the chain. The system is thus in a conventional, homogenously ordered, ferromagnetic phase.

Analogously, if all interactions are smaller than all transverse fields, only sites will be decimated under the renormalization group. Strictly, the interactions need to be smaller than all *fully renormalized* transverse fields in the sense of the adiabatic renormalization of Sec. III C (which also requires sufficiently weak dissipation). This is the conventional paramagnetic phase. As above, there is a finite characteristic energy, viz., the minimum value of the (renormalized) transverse fields in the system.

In the absence of dissipation, these two conventional solutions are gapped, with the energy gap given by the final renormalization-group energy scale discussed above. In the presence of the dissipative baths, a true energy gap does not exist, but the final renormalization-group scale sets a characteristic energy for the magnetic excitations in the system.

After these simple solutions, we now turn our attention to the nontrivial ones at which the interactions J and transverse fields h compete with each other. This means the distributions of the interactions and (renormalized) transverse fields overlap. In these cases, we expect the characteristic renormalization-group energy scale to vanish, either because the system is critical or due to a quantum-Griffiths mechanism. We therefore take $\Gamma \to \infty$ and search for Γ-independent solutions of the rescaled flow equations (27) and (28). In this analysis, we need to distinguish the different types of dissipation.

1. *Review of the dissipationless case*

In the dissipationless case,[11,23] the analysis is simplified by integrating out the magnetic moments. Their distribution can be found separately after the fixed-point distributions $\mathcal{P}^*(\eta)$ and $\mathcal{R}^*_\theta(\theta)$ have been obtained.

There are three types of fixed points.

(i) A critical solution for which duality requires that $f_\zeta = f_\beta$. In order to have a physical (normalizable and nonoscillatory) distribution $\mathcal{P}(\eta)$, we conclude from Eq. (27) that $\dot{f}_\zeta/f_\zeta$ must scale like $1/f_\zeta$ with Γ, implying $f_\zeta \sim \Gamma$.[24] Further analysis (requiring that $\overline{\nu}_0 > 0$) leads to $f_\mu \sim \Gamma^\phi$, with $\phi = (1+\sqrt{5})/2$ being the golden mean. The fixed-point distributions of the rescaled interactions and transverse fields are $\mathcal{P}^*(x) = \mathcal{R}^*_\theta(x) = e^{-x}$. There does not seem to be a simple closed-form expression for the joint fixed-point distribution of fields and moments $\mathcal{R}^*(\theta,\nu)$.

(ii) On the ordered side of the transition, there is a line of fixed points parametrized by $\mathcal{P}_0$ describing the ferromagnetic

quantum Griffiths phase. The scale factors are $f_\zeta = 1$ and $f_\beta = f_\mu = \exp(\mathcal{P}_0\Gamma)$. The fixed-point distributions are given by $\mathcal{P}^*(\eta) = \mathcal{P}_0 e^{-\mathcal{P}_0\eta}$, $\mathcal{R}^*(\theta,\nu) = \mathcal{R}_{\nu,0}\mathcal{R}_{\theta,0} e^{-\mathcal{R}_{\theta,0}\theta}\delta(\mathcal{R}_{\theta,0}\theta - \mathcal{R}_{\nu,0}\nu)$, with $\mathcal{R}_{\theta,0}$ and $\mathcal{R}_{\nu,0}$ being nonuniversal constants (see Appendix).

(iii) Finally, the third type of solution is a line of fixed points on the disordered side of the transition. They are parametrized by $\mathcal{R}_0$ and describe the paramagnetic quantum Griffiths phase. The scale factors are $f_\beta = 1$ and $f_\zeta = \exp(\mathcal{R}_0\Gamma)$. The resulting fixed-point distributions for the interactions and transverse fields read as $\mathcal{P}^*(\eta) = \mathcal{P}_0 e^{-\mathcal{P}_0\eta}$ and $\mathcal{R}^*_\theta(\theta) = \mathcal{R}_0 e^{-\mathcal{R}_0\theta}$ with $\mathcal{P}_0$ a nonuniversal constant. The mean value of the magnetic moments scales as $\overline{\mu} \sim \Gamma$,[11] which suggests that $f_\mu = \Gamma$. However, there is no fixed-point distribution $R^*_\nu(\nu)$.[25] In fact, if one assumes that $\mathcal{R}^*(\theta,\nu)$ exists, one arrives at the incorrect conclusion that $\overline{\mu} = \text{const}$.[23]

2. Super-Ohmic dissipation

To investigate the rescaled flow equations (27) and (28) in the super-Ohmic ($s > 1$) case, we first consider the stability of the dissipationless fixed points of Sec. V C1 with respect to the dissipative terms. In all dissipative terms in Eq. (27) and (28), the dissipation strength α appears in the combination $\alpha f_\mu e^{-(s-1)\Gamma}/f_\beta$. To analyze the behavior of these terms close to the dissipationless fixed points, we use the scale factors f_μ and f_β discussed in Sec. V C1. For all three types of dissipationless fixed points (critical, ferromagnetic Griffiths, and paramagnetic Griffiths), we find that the dissipative terms are subleading and vanish in the limit $\Gamma \to \infty$ for any $s > 1$. This means that the dissipationless fixed points are stable against weak super-Ohmic damping. In other words, super-Ohmic dissipation is an irrelevant perturbation (in the renormalization-group sense) of the dissipationless random transverse-field Ising chain.

We have also checked that the dissipationless fixed-point solutions are the only physical ones by tediously inspecting the flow equations (27) and (28). If we assume that the dissipative terms are the leading ones, we always arrive at unphysical fixed-point distributions.

Instead of reproducing these calculations, we now present a more intuitive argument. β and μ are both renormalized when an interaction is decimated, and both have the same additive recursion relations $\tilde{\beta} = \beta_2 + \beta_3$ and $\tilde{\mu} = \mu_2 + \mu_3$. Therefore, one might expect that $f_\mu \sim f_\beta$. This is not entirely true because β depends explicitly on the value of the renormalization-group scale Γ and thus suffers an additional downward shift of $-d\Gamma$ as the renormalization-group scale is increased from Γ to $\Gamma + d\Gamma$. As a result, f_μ/f_β can diverge in the limit $\Gamma \to \infty$, but never faster than $O(\Gamma)$. Moreover, in the presence of dissipation, integrating out the oscillators via Eq. (11) leads to a downward renormalization of the transverse fields and thus an increase of β. A fixed-point solution then requires a corresponding increase in f_β. It is thus clear that for any physical fixed-point solution of the flow equations (27) and (28), the dissipative terms, which are proportional to $\alpha f_\mu e^{-(s-1)\Gamma}/f_\beta$, remain exponentially suppressed for any $s > 1$.

How do we interpret these results physically? The corrections to the effective transverse fields due to super-Ohmic damping become smaller and smaller with decreasing renormalization-group energy scale Ω and increasing size (magnetic moment) of the clusters. This holds both at criticality and in the surrounding quantum Griffiths phases. The quantum phase transition of the super-Ohmic random transverse-field Ising chain is thus identical to that of the dissipationless chain. Even duality should be recovered at criticality. All these results are in agreement with numerical work in Ref. 17.

3. Ohmic dissipation

In contrast to the super-Ohmic case, Ohmic dissipation is not an irrelevant perturbation. The dissipative terms in the rescaled flow equations (27) and (28) are not exponentially suppressed and become important in *all* of the three regimes (critical, ferromagnetic Griffiths, paramagnetic Griffiths). Hence, qualitatively different behavior is expected.

In this section, we show that the Ohmic dissipation destroys both the paramagnetic quantum Griffiths phase and the quantum critical point. Only a ferromagnetic "Griffiths-type" phase survives. Before discussing the technical details, let us understand this result physically. In a putative paramagnetic quantum Griffiths phase, there are arbitrarily large ferromagnetic clusters embedded in the paramagnetic bulk. As discussed at the end of Sec. IV A, clusters with magnetic moments larger than $\mu_c = \alpha^{-1}$ can never be decimated in the case of Ohmic dissipation. In the low-energy limit, they therefore become frozen and develop true static magnetic order. These static clusters will be aligned by any infinitesimally small interaction, giving rise to long-range order. The system is thus an inhomogeneous ferromagnet rather than a paramagnet.

Let us now see how the same result follows from the flow equations (27) and (28). We start by assuming that there is a paramagnetic quantum Griffiths phase. In such a phase, the majority of renormalization-group steps would be decimations of sites which renormalize the distribution $\mathcal{P}$ of the interactions. The convolution term $\mathcal{P} \overset{\eta}{\otimes} \mathcal{P}$ therefore has to be a leading term in the flow equation (27) to describe the downward flow of the interactions under repeated decimations of sites. Moreover, as $(1 - \alpha\overline{\nu}_0 f_\mu)\mathcal{R}_{\theta,0}$ is the probability for decimating a transverse field, $1 - \alpha\overline{\nu}_0 f_\mu = c$ needs to remain nonzero and positive in the limit $\Gamma \to \infty$. Thus, a physical solution from Eq. (27) requires that f_ζ diverges exponentially and f_β is a constant which we can set to 1. Inserting this into Eq. (28) leads to the fixed-point solution $\mathcal{R}^* = A(\nu)\exp[-c\mathcal{R}^*_{\theta,0}\theta/(1 - \alpha\nu f_\mu)]$, with $A(\nu)$ being a function of ν ensuring normalization and $\mathcal{P}^* = \mathcal{P}_0 \exp(-\mathcal{P}^*_0\eta)$, with $f_\beta = 1$, $f_\mu = \text{const}$, and $f_\zeta = \exp(c\mathcal{R}^*_{\theta,0}\Gamma)$.

However, this solution implies that there are no spin clusters with moments bigger than $\mu_c = \nu_c f_\mu = 1/\alpha$. Thus, this solution can not describe a quantum Griffiths phase in which, due to statistical disorder fluctuations, arbitrarily large magnetic clusters exist with small but nonzero probability. (Whenever the distributions of interactions and transverse fields overlap, it is always possible to find an arbitrarily large region in which all interactions are bigger than all transverse fields.)

Using the same arguments, it also follows that a quantum critical solution of the flow equations (27) and (28) (at which

f_μ has to diverge to reflect the diverging correlation length) can not exist. After having seen that Ohmic dissipation destroys both the paramagnetic quantum Griffiths phase and the quantum critical point (because no physical fixed-point solution is possible when the convolution term $\mathcal{P} \overset{\eta}{\otimes} \mathcal{P}$ is present), we now consider ferromagnetic solutions. On the ferromagnetic side of the transition, almost all renormalization-group steps (at low energies) involve decimations of interactions, while almost no sites are decimated. Therefore, the convolution term $\mathcal{P} \overset{\eta}{\otimes} \mathcal{P}$ drops out of the flow equation for $\Gamma \to \infty$. Moreover, the flow of the interactions close to the fixed point should be analogous to that of the undamped case because their decimations are not influenced by the additional renormalization due to the bosonic baths. Therefore, we use the ansatz $f_\zeta = 1$ as in the undamped case. The flow equation (27) then yields

$$\mathcal{P}^*(\eta) = \mathcal{P}_0 e^{-\mathcal{P}_0 \eta}, \tag{29}$$

where $\mathcal{P}_0$ is a nonuniversal constant which parametrizes the line of ferromagnetic fixed points.

Let us now turn our attention to the joint distribution $\mathcal{R}^*(\theta,\nu)$ of transverse fields and magnetic moments at these fixed points. In the dissipationless case (Sec. V C1), fields and moments rescale in the same way, $f_\mu = f_\beta$. In the presence of Ohmic dissipation, the transverse fields suffer additional downward renormalizations due to Eq. (11), which become more and more important as larger ferromagnetic clusters are formed with increasing Γ. We thus expect that $f_\mu/f_\beta \to 0$ with $\Gamma \to \infty$. Under this assumption, the flow equation (28) greatly simplifies, and all dissipative terms drop out. This implies that the functional form of the fixed-point distribution in terms of θ and ν is identical to that of the undamped system in the ferromagnetic quantum Griffiths phase. As in Ref. 11, we can integrate over either ν or β and analyze the resulting reduced distributions $\mathcal{R}^*_\theta$ and $\mathcal{R}^*_\nu$. This yields the fixed-point distributions $\mathcal{R}^*_\theta = \mathcal{R}_{\theta 0} e^{-\mathcal{R}_{\theta 0}\theta}$ and $\mathcal{R}^*_\nu = \mathcal{R}_{\nu 0} e^{-\mathcal{R}_{\nu 0}\nu}$, just as in the undamped case.

To fix the free parameters $\mathcal{R}_{\theta 0}$ and $\mathcal{R}_{\nu 0}$ and to find the joint distribution $\mathcal{R}^*(\theta,\nu)$, we need to take into account the subleading term in the flow equation (28) close to the fixed point. In contrast to the leading terms, the subleading ones do depend on the dissipation. The details of this somewhat lengthy analysis are presented in Appendix. We find $f_\mu = e^{\mathcal{P}_0\Gamma}$ and $f_\beta = \Gamma e^{\mathcal{P}_0\Gamma}$ as well as $\mathcal{R}_{\nu 0}/\mathcal{R}_{\theta 0} = \alpha$. Moreover, the rescaled magnetic moments and transverse fields become perfectly correlated at the fixed point, such that the joint distribution reads as

$$\mathcal{R}^*(\beta,\nu) = \mathcal{R}_0 e^{-\mathcal{R}_0\nu}\delta(\theta - \alpha\nu). \tag{30}$$

The remaining nonuniversal constant $\mathcal{R}_0$ depends on the initial conditions.

To summarize, instead of a quantum critical fixed point accompanied by lines of quantum Griffiths fixed points on each side of the transition, we only find a ferromagnetic solution that describes the physics for all overlapping distributions of interactions and renormalized transverse fields. To test the stability of this fixed point, we have computed closed-form solutions of the entire renormalization-group flow for some particularly simple initial distributions of transverse fields and interactions (see Appendix. In addition, we have implemented the recursion relations numerically[25,26] and verified that the distributions flow toward our fixed point for many different initial distributions.

4. *Sub-Ohmic dissipation*

For the sub-Ohmic random transverse-field Ising chain, our strong-disorder renormalization-group method can not be applied because the adiabatic renormalization of the field does not capture all of the relevant physics of the problem. In the sub-Ohmic case, the adiabatic renormalization only works in the limit of weak transverse fields.[12] In this limit, the dissipation suppresses the tunneling for any dissipation strength α. This means the transverse fields all renormalize to zero for any α. Thus, within the adiabatic renormalization approach to the baths, the sub-Ohmic random transverse-field Ising chain does not have a quantum phase transition, and it is always in the ferromagnetic ground state.

However, it is known from more advanced techniques that the sub-Ohmic spin-boson model with fixed weak dissipation does undergo a quantum phase transition at some nonzero value of the transverse field (see, e.g., Refs. 27 and 28). In our context, this implies that small clusters fluctuate, but the dynamics of sufficiently large clusters freezes (their transverse fields vanish under renormalization) just like in the Ohmic case. We will briefly discuss the resulting behavior in Sec. VII.

VI. PHASE DIAGRAM AND OBSERVABLES

Using the fixed-point distributions found in Sec. V, we can now determine the phase diagram and compute thermodynamic observables close to the quantum phase transition.

A. Phase diagram and crossovers

Let us contrast the infinite-randomness critical-point scenario of the dissipationless random transverse-field Ising chain[10,11] (which, according to Sec. V C2, also applies to super-Ohmic damping) with the smeared-transition scenario emerging for Ohmic dissipation. The phase diagram of the dissipationless case as function of temperature T and typical transverse field $h_{\rm typ}$ is sketched in Fig. 3(a) (keeping the typical interaction strength fixed).

At zero temperature, the ferromagnetic-paramagnetic quantum phase transition is governed by a universal infinite-randomness fixed point (IRFP). It is accompanied on both sides by the gapless paramagnetic (weakly disordered) and ferromagnetic (weakly ordered) quantum Griffiths phases. For higher fields (to the right of the paramagnetic Griffiths phase), there is a conventional (strongly disordered) gapped quantum paramagnet where quenched disorder effects are irrelevant. For sufficiently weak fields (to the left of the ferromagnetic Griffiths phase), the system is a conventional (strongly ordered) gapped ferromagnet where quenched disorder is also irrelevant.

As ferromagnetic order in one dimension is destabilized at any nonzero temperature, only crossovers will occur for $T > 0$ [as depicted by the dashed lines in Fig. 3(a)]. Above the critical point, there is the quantum critical region, which is characterized by activated scaling, i.e., the dynamical exponent is formally infinity. If the system is close to but not at the

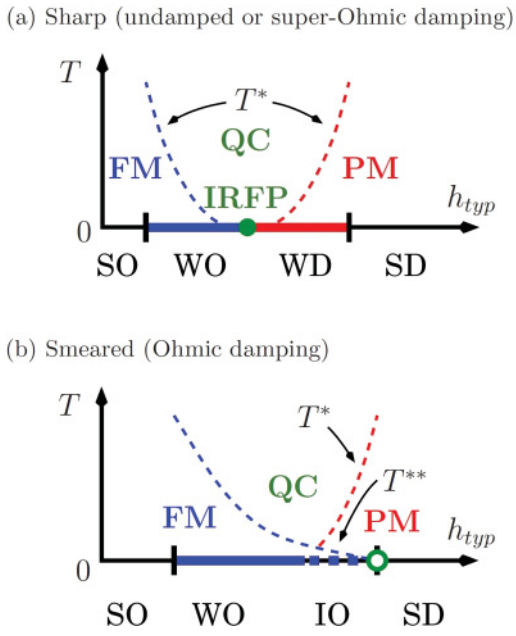

FIG. 3. (Color online) Schematic phase diagrams in the transverse-field ($h_{\rm typ}$) temperature (T) plane. (a) Infinite-randomness critical-point scenario of the dissipationless and super-Ohmic chains. SO and SD denote the strongly ordered and disordered conventional phases, while WO and WD denote the ordered and disordered quantum Griffiths phases. (b) Smeared-transition scenario for Ohmic dissipation ($0 < \alpha \ll 1$), with the inhomogeneously ordered (IO) ferromagnet replacing the WD Griffiths phase. The open circle marks the end of the tail of the smeared transition. The thin dashed lines represent finite-temperature crossovers between a quantum critical (QC) regime and a quantum paramagnet (PM) or ferromagnet (FM). The crossover temperatures T^* and T^{**} are discussed in the text.

quantum critical point, it undergoes a crossover to one of the quantum Griffiths phases upon lowering the temperature. In these phases, the dynamical scaling is conventional, i.e., the dynamical exponent is finite, $z \sim 1/|r|$, where $r = h_{\rm typ} - h_c$ is the distance from criticality and h_c is the critical field. In the undamped case, duality requires the critical point to occur when the typical interactions equal the typical transverse fields, thus $h_c = J_{\rm typ}$. For super-Ohmic dissipation, the fields are renormalized downward by the oscillators. Using Eq. (10), we find $h_c \approx J_{\rm typ} \exp\{\alpha/(s-1)\}$. The crossover temperature T^* is obtained from the activated dynamical scaling at the IRFP,

$$T^* \sim \exp(-\text{const}/|r|^{-\nu\psi}), \tag{31}$$

where $\nu = 2$ and $\psi = 1/2$ are the correlation length and tunneling exponents of the IRFP, respectively, and the constant is of order unity.

Having reviewed the undamped case, let us now discuss the case of Ohmic dissipation. For weak damping $\alpha \ll 1$, the renormalization-group flow at high energies (where all clusters are still small) will be almost identical to that of the undamped system. Thus, the high-temperature part of the phase diagram shown in Fig. 3(b) is analogous to its undamped counterpart. However, upon lowering the energy scale (i.e., the temperature), the clusters grow. In the undamped quantum Griffiths paramagnet discussed above, their average magnetic moment grows as $\overline{\mu} \sim r^{\nu\psi(1-\phi)} \ln(\Omega_I/T)$, with $\phi = (1+\sqrt{5})/2$, and at the quantum critical point it increases as $\overline{\mu} \sim [\ln(\Omega_I/T)]^{\phi}$.[11] Therefore, it is clear that at some crossover temperature T^{**}, the cluster moment reaches the critical value $\mu_c = 1/\alpha$, and dissipation becomes important. The value of T^{**} can be estimated from the condition $\overline{\mu} = 1/\alpha$; this gives

$$T^{**} \sim \exp[-\text{const} \times (1/\alpha)^{1/\phi}] \tag{32}$$

very close the quantum critical point of the undamped system, and

$$T^{**} \sim \exp(-\text{const} \times r^{\nu\psi(\phi-1)}/\alpha) \tag{33}$$

for larger transverse fields.

At temperatures below T^{**}, the quantum dynamics of the surviving clusters freezes completely (because their renormalized transverse fields vanish). These clusters thus behave like large *classical* spins. At zero temperature, they can be aligned by any infinitesimally weak interaction, leading to long-range order. Thus, the quantum Griffiths paramagnet (and quantum critical point) are replaced by an inhomogeneously ordered (IO) ferromagnetic phase [marked by the thick dashed line in Fig. 3(b). This phase is due to *local* formation of magnetic order rather than a collective effect, which implies that the paramagnetic-ferromagnetic quantum phase transition is smeared. It also means that the end point of the tail of the smeared transition [marked by the open circle in Fig. 3(b)] is *not* a critical point.

B. Observables

We now turn our attention to observables. As shown in Sec. V C2, super-Ohmic dissipation is an irrelevant perturbation at the infinite-randomness critical point of the dissipationless random transverse-field Ising chain. Therefore, the low-energy behavior of observables in the super-Ohmic case is identical to that in the dissipationless case, which is discussed in detail in Ref. 11 (see also Ref. 22 for a review of additional results). This observation agrees with numerical results of Schehr and Rieger.[17]

Here, we therefore only consider the case of Ohmic dissipation. Moreover, we focus on the inhomogeneously ordered (IO) ferromagnetic phase (i.e., on the tail of the smeared transition), which is the novel feature of the Ohmic chain. As we have seen in the analysis of the flow equations in Sec. V, weak dissipation does not change the behavior of the other phases qualitatively; it only leads to quantitative corrections to the undamped physics.

To characterize the extent to which the bare (initial) distributions P_I and R_I of the interactions and transverse fields overlap, we introduce the probability of an interaction J being larger than a renormalized transverse field

$$w = \int_0^\infty dJ\, P_I(J) \int_0^J dh_{\rm eff} R_I(h_{\rm eff}), \tag{34}$$

where $h_{\rm eff} = h(h/\Omega_I)^{\alpha/(1-\alpha)}$ is a local field fully renormalized by the baths according to Eq. (11). If $w = 1$, all interactions are larger than all fields, and the system is in the conventional (strongly ordered) ferromagnetic phase. Conversely, if $w = 0$, all interactions are weaker than all transverse fields,

putting the system in the conventional (strongly disordered) paramagnetic phase. Rare regions exist for $0 < w < 1$ with the inhomogeneously ordered regime (the tail of the smeared transition) corresponding to $w \ll 1$.

To leading approximation, the zero-temperature spontaneous magnetization m is simply the magnetic moment of the last spin cluster remaining after the renormalization-group energy scale Ω has been iterated to zero. In the tail of the smeared transition $w \ll 1$, this cluster is made up of a collection of well-separated rare regions of minimum moment $1/\alpha$ on which the interactions are larger than the transverse fields. The probability for finding a rare region of $1/\alpha$ sites is simply $w^{1/\alpha}$. We thus conclude that the magnetization in the tail of the smeared transition $w \ll 1$ behaves as

$$m \sim w^{1/\alpha}. \tag{35}$$

Note that this result implies that the dependence of the magnetization on the typical transverse-field strength $h_{\rm typ}$ is nonuniversal; it depends on the details of the bare distributions P_I and R_I. This nonuniversality agrees with heuristic results on other smeared phase transitions.[15,29–31]

For weak dissipation and close to the location of the undamped quantum critical point, the magnetization can also be estimated by the fraction of undecimated spins when the undamped renormalization-group flow reaches the crossover energy scale T^{**} (because below T^{**} almost no sites will be decimated). This can be readily accomplished using the results of Ref. 11. The fraction of undecimated spins at scale T^{**} is given roughly by the product of the density of surviving clusters at this scale $n(T^{**})$ and their moment $\overline{\mu}(T^{**})$. As the moment is simply $1/\alpha$ (from the definition of T^{**}), we obtain

$$m \sim \alpha^{1/(\phi\psi)-1} \tag{36}$$

at the undamped quantum critical point, and

$$m \sim \alpha^{-1} r^{\nu} \exp(-\text{const} \times r^{1+\nu\psi(\phi-1)}/\alpha) \tag{37}$$

on its paramagnetic side. On the ferromagnetic side, the magnetization is nonzero even in the absence of damping; weak dissipation thus provides a small correction only. The result (37) holds sufficiently close to the undamped quantum critical point. As the paramagnetic phase is approached for larger r, the behavior crosses over to Eq. (35) (see also Fig. 1 of Ref. 18).

The (order-parameter) magnetic susceptibility χ can be computed by performing the renormalization group until the energy scale Ω reaches the temperature T. All spins decimated in this process are rapidly fluctuating between up and down (i.e., pointing in the x direction due to their strong transverse field) and contribute little to the susceptibility. All clusters remaining at scale T are treated as free and contribute a Curie term μ^2/T to the susceptibility.

For temperatures above T^{**}, the renormalization-group flow coincides with that of the undamped case. The temperature dependence of the susceptibility is therefore identical to that of the dissipationless transverse-field Ising chain.[11] In particular, in the quantum critical region, χ increases as

$$\chi \sim n(T)\overline{\mu}^2(T)/T \sim [\ln(\Omega_I/T)]^{2\phi-1/\psi}/T, \tag{38}$$

with vanishing T. In the paramagnetic Griffiths region, it behaves as

$$\chi \sim r^{\nu+2\nu\psi(1-\phi)}[\ln(\Omega_I/T)]^2\, T^{-1+1/z}, \tag{39}$$

with $z \approx 1/(2r)$ being the dynamical exponent.

Below T^{**}, the renormalization-group flow deviates from the undamped one, and the system crosses over into the inhomogeneously ordered (IO) ferromagnetic phase. Here, the susceptibility can be calculated from the fixed-point solution of Sec. V C3. Following the same steps as in the *ferromagnetic* Griffiths phase of the undamped system, we obtain

$$\chi \sim T^{-1-1/z'}, \tag{40}$$

with $z' = 1/\mathcal{P}_0$ being the low-energy dynamical exponent in the ferromagnetic phase [see Eq. (29)].

It is desirable to relate the dynamical exponent z' of the inhomogeneous ferromagnet to the bare distributions of J and h, or to the distance r from the undamped quantum critical point. The qualitative behavior is easily discussed. On the ferromagnetic side of the undamped transition ($r < 0$), z' approximately agrees with its undamped value because dissipation is a subleading correction, hence, $z' \approx z \approx -1/(2r)$. In the inhomogeneously ordered phase (i.e., on the paramagnetic side of the undamped transition $r > 0$), $\mathcal{P}_0$ is determined by the distribution of the interactions between the surviving clusters at energies below T^{**}. With increasing transverse fields (increasing r), these clusters become rarer, implying that the distribution of their interactions becomes broader. Thus, $\mathcal{P}_0$ decreases with increasing transverse fields in the tail of the smeared transition. In the far tail $w \ll 1$, the clusters surviving at energy scale T^{**} are essentially independent, which means that their distances follow a Poisson distribution of width $w^{-1/\alpha}$. This translates into the exponential distribution (29) of the coupling variables η, with $\mathcal{P}_0 \sim w^{1/\alpha}$. Thus, the dynamical exponent

$$z' = 1/\mathcal{P}_0 \sim w^{-1/\alpha} \tag{41}$$

diverges at the endpoint of the tail where $w = 0$.

Close to the undamped quantum critical point, the behavior of z' can also be determined from the undamped renormalization-group flow. We approximate the flow in the Griffiths paramagnet by disregarding the effects of dissipation until we reach the energy scale of T^{**}. Below this scale, we assume that no further field decimations are performed. The value of the parameter $\mathcal{P}_0$ can then be obtained from the distribution $\mathcal{P}$ of the undamped Griffiths paramagnet at the energy scale $\Gamma^{**} = \ln(\Omega_I/T^{**})$. This yields

$$z' \sim \frac{1}{r} \exp[\text{const} \times r^{\psi\nu(\phi-1)+1}/\alpha]. \tag{42}$$

Thus, z' increases with increasing r, in agreement with the above heuristic arguments. Our results for z' imply a dramatic change of the dynamical exponent when crossing over from the quantum Griffiths paramagnet to the inhomogeneously ordered ferromagnet at T^{**}. Such behavior was indeed observed by means of a numerical implementation of the renormalization-group rules.[25,26]

VII. DISCUSSION

A. Applicability to weakly disordered systems

In this section, we discuss to what extent our results apply to systems with weak or moderate bare disorder. The strong-disorder renormalization-group recursion relations derived in Sec. III become asymptotically exact in the limit of infinite disorder, but they are only approximations for finite disorder. For this reason, the strong-disorder renormalization group needs to be complemented by other methods to discern the fate of weakly disordered systems.

To analyze the limit of weak disorder, we can start from the Harris criterion,[3] which states that a clean critical point is stable against weak disorder if its correlation length exponent ν fulfills the inequality $d\nu > 2$. The clean Ohmic transverse-field Ising chain features a quantum critical point with an exponent value $\nu \approx 0.638$.[32] Disorder is thus a relevant perturbation. Kirkpatrick and Belitz[33] and Narayanan *et al.*[34,35] studied a quantum order-parameter field theory with Ohmic dissipation by means of a conventional perturbative renormalization group. This method, which is controlled at *weak* disorder, did not produce a stable critical fixed point, but runaway flow toward large disorder (where the strong-disorder renormalization group becomes better and better). This strongly suggests that our results apply for any amount of (bare) disorder.

We now turn to the question of whether or not our results become asymptotically exact in the low-energy limit. To address this question, we need to discuss the widths of the distributions π and ρ of the logarithmic interaction and transverse-field variables in the inhomogeneously ordered ferromagnet. Using the fixed-point distributions (29) and (30) and the corresponding scale factors $f_\zeta = 1$ and $f_\beta = \Gamma e^{\mathcal{P}_0\Gamma}$, we find the widths to be given by $1/\pi_0 = 1/\mathcal{P}_0$ and $1/\rho_{\beta,0} = \Gamma e^{\mathcal{P}_0\Gamma}/\mathcal{R}_{\theta,0}$. Thus, the relative width of the transverse-field distribution diverges, while the width of the interaction distribution remains finite in the limit $\Gamma \to \infty$ ($\Omega \to 0$).

This result can be easily understood by following the renormalization-group flow. Above the crossover energy scale Ω^{**} (where the typical cluster size reaches $1/\alpha$), the flow approximately coincides with that of a paramagnetic Griffiths phase of the undamped problem. Thus, (almost) only sites are decimated, which enormously broadens the distribution π of the interactions. Below Ω^{**}, almost all decimations are interaction decimations. Therefore, π does not renormalize further, and its width remains large but finite. In contrast, the transverse fields are driven to zero and their distribution broadens without limit. Our results for the inhomogeneously ordered ferromagnet are thus not asymptotically exact, but represent a good approximation. However, in the tail of the smeared transition $w \to 0$, the width of the interaction distribution diverges [see Eqs. (41) and (42)].

In this large-disorder limit, higher-order corrections to the recursion relations derived in Sec. III are suppressed. This includes couplings between different dissipative baths that appear upon integrating out a site. As these couplings only appear in fourth order of perturbation theory, they are very weak (and of short-range type) in the large-disorder limit. Thus, all corrections to our recursion relations are irrelevant in the renormalization-group sense, and our theory becomes asymptotically exact in the tail of the smeared transition.

Finally, we discuss to what extent our results would change if the bare system had long-range interactions between the different baths (or equivalently, a single global bath). In this case, the true zero-temperature behavior would be dominated by these interactions and differ from our results. However, sufficiently weak long-range couplings would become important only at very low temperatures [below even T^{**}, see Fig. 3(b)]. Thus, our theory would remain valid in a broad temperature window. The precise value of the crossover energy scale depends on the bare value of the long-range interactions and on in the details of the model. It is a nonuniversal quantity and beyond the scope of this work.

B. Sub-Ohmic dissipation

As discussed in Sec. V C4, our strong-disorder renormalization-group method can not be directly applied to the sub-Ohmic case because there is no phase transition if the dissipative baths are treated within adiabatic renormalization. However, a qualitative picture of the physics of the sub-Ohmic case can nonetheless be developed.

The sub-Ohmic spin-boson model is known[27,28] to undergo a continuous quantum phase transition from a fluctuating phase to a localized (frozen) phase as the transverse field is decreased (or the dissipation strength increased). Thus, the dynamics of sufficiently large spin clusters (which have small effective transverse fields and large dissipation strength) is always frozen. These frozen (classical) clusters can be aligned by any infinitesimal interaction, leading to magnetic long-range order. Just as in the Ohmic case, this mechanism replaces the paramagnetic Griffiths phase and the quantum critical point by an inhomogeneously ordered ferromagnetic phase and smears the underlying ferromagnetic quantum phase transition.

C. Higher dimensions

We now discuss to what extent our results also apply to dissipative random transverse-field Ising models in higher space dimensions. The renormalization-group steps of Sec. III can be performed in complete analogy to the one-dimensional case, and the resulting recursion relations take the same form as Eqs. (11), (12), (14), and (15). However, decimating a site now generates effective interactions between all pairs of its neighboring sites, while decimating an interaction leads to an effective site (cluster) that couples to a larger number of neighbors than before. Thus, both decimation steps change the connectivity of the lattice. Moreover, they introduce correlations between the remaining couplings. For this reason, an analytical treatment of the renormalization-group flow appears to be impossible, even in the dissipationless case. However, the strong-disorder renormalization group has been implemented numerically in two and higher dimensions by keeping track of the irregular "maze" of new interactions created by the decimation steps.[36,37] An analogous approach would be possible in the dissipative case.

Even in the absence of a complete solution, the effects of dissipation on higher-dimensional random transverse-field Ising models can be understood qualitatively. The extra

downward renormalization (11) of the transverse fields due to the baths is purely local, and thus also applies to higher dimensions. Just as in one dimension, it reduces the probability of decimating a site, $(1-\alpha\overline{\mu}_{\Omega})R_h(\Omega)$. Once the moment μ of a cluster reaches $1/\alpha$, it will never be decimated. We conclude that clusters with moments $\mu > 1/\alpha$ will freeze, implying that a critical fixed-point solution is impossible. As in one dimension, the quantum phase transition is therefore smeared, and the paramagnetic Griffiths phase is replaced by an inhomogeneously ordered ferromagnetic phase.

Although the zero-temperature quantum phase transition of the higher-dimensional random transverse-field Ising models is similar to the one-dimensional case, their behavior at nonzero temperatures differs. In one dimension, long-range order only exists at zero temperature (see our phase diagrams, Fig. 3). In higher dimensions, a long-range ordered ferromagnetic phase can exist at nonzero temperatures. It is important to note that the classical phase transition separating this phase from the paramagnet at nonzero temperatures is *not* smeared. At nonzero temperatures, even the largest clusters (rare regions) will thermally fluctuate. Thus, a finite interaction is required to align them. This restores a sharp phase transition.[15]

In two or more space dimensions, disorder can also be introduced into the (dissipationless) transverse-field Ising model simply by diluting the lattice. For weak transverse fields, the ferromagnetic phase survives up to the percolation threshold p_c of the lattice. The quantum percolation phase transition emerging at p_c shares many characteristics with the infinite-randomness critical points of the generic random transverse-field Ising models.[38] Adding Ohmic dissipation suppresses the quantum fluctuations of sufficiently large percolation clusters. The result is an unusual classical superparamagnetic phase.[39] However, the percolation transition remains sharp as it is driven by the critical lattice geometry at the percolation threshold.

D. Experiments

To the best of our knowledge, an experimental realization of the *microscopic* Hamiltonian defined in Eqs. (1) to (4) has not been found yet. However, its order-parameter field theory, a one-component ϕ^4 theory with an inverse Gaussian propagator of the form $G(\mathbf{q},\omega)^{-1} = r + \mathbf{q}^2 + |\omega|^s$, also describes a number of experimentally important quantum phase transitions. Based on universality, we expect the qualitative properties of these transitions to be analogous to those of our model (1).

For example, Hertz' theory[40] of the antiferromagnetic quantum phase transition of itinerant electrons leads to such an order-parameter field theory. In this case, the dissipation is Ohmic ($s = 1$); it is caused by the electronic particle-hole excitations rather than abstract heat baths. For disordered itinerant ferromagnets, the dynamic part of the Gaussian propagator takes the form $|\omega|/\mathbf{q}^2$ rather than $|\omega|$. Experiments on these disordered metallic quantum magnets often show unusual behavoir,[41–43] and strong-disorder effects have been suggested as possible reasons.[44] However, explicit verifications of the quantum Griffiths and smeared-transition scenarios were missing for a long time. Only recently, some promising results have been found in several itinerant ferromagnets.[45–47] For a more thorough discussion, the reader is referred to Refs. 48 and 49.

We emphasize that even though the leading terms in the order-parameter field theory of the dissipative random transverse-field Ising model (1) agree with the corresponding terms in itinerant quantum magnets, their behaviors are not completely identical. Importantly, in the Hamiltonian (1), each spin couples to its own independent dissipative bath. In contrast, in metallic magnets, all spins couple to the same Fermi sea. This produces an additional long-range interaction between the spins which has no counterpart in the Hamiltonian (1). It is mediated by the fermionic particle-hole excitations and known as the Ruderman-Kittel-Kasuya-Yosida (RKKY) interaction.

VIII. CONCLUSIONS

To summarize, we have studied the quantum phase transition of the dissipative random transverse-field Ising chain via an analytical implementation of a strong-disorder renormalization-group method. We have shown that super-Ohmic dissipation is an irrelevant perturbation. The quantum phase transition is thus in the same universality class as the dissipationless chain, i.e., it is governed by an infinite-randomness fixed point and accompanied by quantum Griffiths singularities.

In contrast, for Ohmic dissipation, the sharp quantum phase transition is destroyed by smearing because sufficiently large rare regions completely freeze at zero temperature. Note that this as a consequence of the *interplay* between disorder and dissipation as neither disorder nor dissipation alone can smear the quantum phase transition of the transverse-field Ising chain. The behavior of the sub-Ohmic case is qualitatively similar to the Ohmic one: it also leads to a smeared transition.

The results of this paper apply to the case of discrete Ising order-parameter symmetry. Systems with continuous $O(N)$ order-parameter symmetry behave differently. In contrast to sufficiently large Ising clusters, which freeze in the presence of Ohmic dissipation, $O(N)$ clusters of all sizes continue to fluctuate with a rate that depends exponentially on their magnetic moment.[50] The resulting sharp phase transition is controlled by an infinite-randomness critical point in the universality class of the undamped random transverse-field Ising model.[51,52] Super-Ohmic dissipation has weaker effects,[53] and the renormalization-group flow is very similar to the dissipationless case.[54]

The difference between the discrete and continuous symmetry cases as well as the differences between the different types of dissipation can all be understood in terms of a classification of rare-region effects according to the effective defect (rare-region) dimensionality:[48,50] If the rare-region dimensionality d_{RR} is below the lower critical dimension d_c^- of the problem at hand, the transition is sharp and conventional. If $d_{RR} = d_c^-$, the transition is still sharp but controlled by an infinite-randomness critical point. Finally, if finite-size rare regions can order independently of each other ($d_{RR} \geqslant d_c^-$), the transition is smeared. This classification applies to classical phase transitions and to quantum phase transitions that can be related to classical ones via the quantum-to-classical mapping.[55]

We expect our work or appropriate generalizations to shed light onto a variety of quantum phase transitions in disordered systems in which the order-parameter modes are coupled to additional noncritical soft modes.

ACKNOWLEDGMENT

This work has been supported in part by the NSF under Grant No. DMR-0906566, Research Corporation, FAPESP under Grant No. 2010/03749-4, and CNPq under Grants No. 590093/2011-8 and No. 302301/2009-7.

APPENDIX: RENORMALIZATION-GROUP FLOW IN THE OHMIC FERROMAGNETIC PHASE

In this appendix, the flow equations (27) and (28) are studied in the ferromagnetic regime for Ohmic ($s = 1$) damping. For ferromagnetic fixed-point solutions, the convolution term in (27) has to drop out, leading to

$$0 = \frac{\dot{f}_\zeta}{f_\zeta}\left(\mathcal{P} + \eta\frac{\partial \mathcal{P}}{\partial \eta}\right) + \frac{1}{f_\zeta}\left(\frac{\partial \mathcal{P}}{\partial \eta} + \mathcal{P}_0\mathcal{P}\right). \tag{A1}$$

As no sites are decimated, the typical value of ζ can not grow (as in the undamped case). Thus, $f_\zeta = 1$ and

$$\mathcal{P}^*(\eta) = \mathcal{P}_0 e^{-\mathcal{P}_0\eta}, \tag{A2}$$

with $\mathcal{P}_0$ being an integration constant. With $f_\zeta = 1$ and assuming that

$$f_\mu/f_\beta \to 0 \tag{A3}$$

(because we expect that f_β grows faster than f_μ due to the dissipation), the fixed-point equation (28) reads as

$$0 = \frac{\dot{f}_\beta}{f_\beta}\left(\mathcal{R} + \theta\frac{\partial \mathcal{R}}{\partial \theta}\right) + \frac{\dot{f}_\mu}{f_\mu}\left(\mathcal{R} + \nu\frac{\partial \mathcal{R}}{\partial \nu}\right) + \mathcal{P}_0(\mathcal{R} \overset{\theta,\nu}{\otimes} \mathcal{R} - \mathcal{R}). \tag{A4}$$

Interestingly, all dissipative terms (those involving α) drop out, and we recover the undamped fixed-point equation. Therefore, we can integrate either over the fields or over the magnetic moments and analyze $\mathcal{R}_\theta$ or $\mathcal{R}_\nu$ separately. Physically relevant solutions require that all terms in Eq. (A4) survive in the limit $\Gamma \to \infty$, which implies $\dot{f}_\beta/f_\beta = \dot{f}_\mu/f_\mu = \text{const}$. Integrating over ν and Laplace transforming (A4), we arrive at

$$0 = -cz\frac{\partial}{\partial z}\hat{\mathcal{R}}^*(z,0) + \mathcal{P}_0\hat{\mathcal{R}}^*(z,0)(\hat{\mathcal{R}}^*(z,0) - 1), \tag{A5}$$

where $\hat{\mathcal{R}}(v,n) = \int_0^\infty e^{-v\theta - n\nu}\mathcal{R}(\theta,\nu)d\theta\, d\nu$ and $c \geqslant \mathcal{P}_0$ is a constant. Equation (A5), which can be linearized via $\hat{\mathcal{R}}^* = -c(\partial_{\ln v}\ln u)/\mathcal{P}_0$, then yields

$$\hat{\mathcal{R}}^*(v,0) = \frac{1}{1 + (v/A)^{\mathcal{P}_0/c}}, \tag{A6}$$

where A is an integration constant. For $c \neq \mathcal{P}_0$, the inverse Laplace transformation gives $\mathcal{R}^*_\theta(\theta) \propto \theta^{-1-\mathcal{P}_0/c}$ for $\theta \gg 1$, which corresponds to $R^*_h(h) \sim 1/(h|\ln h|^{1+\mathcal{P}_0/c})$ for $h \ll 1$. Although this extremely singular distribution is a fixed-point solution of the flow equations, it is *not* the attractive one for typical initial distributions. Indeed, this extreme fixed point can only be accessed if the *bare* distribution of fields already contains such strong singularity.[11]

The less singular (and attractive) solutions correspond to $c = \mathcal{P}_0$. By inverse Laplace transforming (A6), we conclude that $\mathcal{R}^*_\theta = \mathcal{R}_{\theta 0}e^{-\mathcal{R}_{\theta 0}\theta}$, which is identical to the undamped case.[11] The same analysis applies to $\mathcal{R}^*_\nu = \mathcal{R}_{\nu 0}e^{-\mathcal{R}_{\nu 0}\nu}$. Here, $\mathcal{R}_{\theta 0}$ and $\mathcal{R}_{\nu 0}$ are nonuniversal constants. Moreover, since the flow of the magnetic moments is identical to the undamped case, we conclude that $f_\mu = e^{\mathcal{P}_0\Gamma}$. Recall we can not use the result of the undamped case in which $f_\beta = f_\mu$ because of our assumption (A3).

After finding the reduced fixed-point distributions $\mathcal{R}^*_\theta$ and $\mathcal{R}^*_\nu$, we now search for the joint fixed-point distribution $\mathcal{R}^*(\theta,\nu)$ with $\dot{f}_\beta/f_\beta = \dot{f}_\mu/f_\mu = \mathcal{P}_0$ and $f_\mu/f_\beta = 0$ in the limit $\Gamma \to \infty$. The Laplace-transformed flow equation (A4) becomes

$$0 = -v\frac{\partial \hat{\mathcal{R}}}{\partial v} - n\frac{\partial \hat{\mathcal{R}}}{\partial n} + \hat{\mathcal{R}}(\hat{\mathcal{R}} - 1), \tag{A7}$$

which can be linearized via $\hat{\mathcal{R}} = -\partial_m \ln u$, where $m = \ln v + \ln n$. Hence,

$$\hat{\mathcal{R}}^*(v,n) = [1 + f(v/n)\sqrt{vn}]^{-1}, \tag{A8}$$

where $f(k)$ is a generic function constrained to diverge $\sim\sqrt{k}/\mathcal{R}_{\theta 0}$ when $k \to \infty$, and to diverge $\sim 1/(\sqrt{k}\mathcal{R}_{\nu 0})$ when $k \to 0$ as dictated by the solution (A6).

Our purpose now is to find the correct function $f(k)$ in Eq. (A6). It is easy to see that there are two limiting cases of the joint distribution $\mathcal{R}(v,n)$ that are compatible with the reduced distributions $\mathcal{R}^*_\theta$ and $\mathcal{R}^*_\nu$ found above, viz.,

$$\hat{\mathcal{R}}_{\text{corr}}(v,n) = \left(1 + \frac{v}{R_{\theta 0}} + \frac{n}{R_{\nu 0}}\right)^{-1} \tag{A9}$$

and

$$\hat{\mathcal{R}}_{\text{uncorr}}(v,n) = \left(1 + \frac{v}{R_{\theta 0}}\right)^{-1}\left(1 + \frac{n}{R_{\nu 0}}\right)^{-1}, \tag{A10}$$

which, respectively, correspond to perfect correlations $\mathcal{R}_{\text{corr}}(\theta,\nu) = R_{\theta 0}R_{\nu 0}e^{-R_{\theta 0}\theta}\delta(R_{\theta 0}\theta - R_{\nu 0}\nu)$, and no correlations $\mathcal{R}_{\text{uncorr}}(\theta,\nu) = R_{\theta 0}e^{-R_{\theta 0}\theta}R_{\nu 0}e^{-R_{\nu 0}\nu}$, between transverse fields and magnetic moments. However, $\hat{\mathcal{R}}_{\text{uncorr}}$ does *not* satisfy the general form (A8). This suggests that correlations between the fields and magnetic moments arise from the fixed-point structure itself, regardless the strength of the damping α. Indeed, as we shall see below, the flow is toward the perfect correlated case (A9).

Since it is not possible to gather full information about $f(v/n)$ by analyzing the fixed-point solution alone, we now analyze the renormalization-group flow near the fixed point. This can only be accomplished if the Γ dependence is not scaled out. We thus consider the unscaled variables β and μ and use the fixed point (A8) as reference. Having in mind that $f_\mu = e^{\mathcal{P}_0\Gamma}$, $f_\mu/f_\beta \to 0$, and $\dot{f}_\beta/f_\beta \to \mathcal{P}_0$, we keep only the main terms as well as the leading corrections in the flow equation (26):

$$\frac{\partial \rho}{\partial \Gamma} = -\alpha\mu\frac{\partial \rho}{\partial \beta} + \pi_0(\rho \otimes \rho - \rho). \tag{A11}$$

It is easy to see that the neglected term corresponds to the third one on the right-hand side of Eq. (28), which is the

one responsible for the normalization of $\mathcal{R}$ due to a field decimation. The effects of damping thus enter only in the renormalization of the fields upon cooling the bath.

The careful reader may notice that the neglected term is proportional to f_μ/f_β as is the fourth one. Then, why is $-\alpha\overline{\mu}_0\rho_{\beta,0}\rho$ neglected and $-\alpha\mu\partial\rho/\partial\beta$ is not? The reason comes from the arising correlations between transverse fields and magnetic moments. Consider for instance the perfectly correlated case $\mathcal{R}_{\rm corr}$. With this choice,

$$\overline{\mu}_0 = f_\mu\overline{\nu}_0 = f_\mu\frac{\int \nu\mathcal{R}_{\rm corr}(0,\nu)d\nu}{\int \mathcal{R}_{\rm corr}(0,\nu)d\nu} = 0.$$

This result is interesting because, as argued in Sec. IV, $(1-\alpha\overline{\mu}_0\rho_{\beta,0})\rho$ is the probability of having a decimation of a field. Since the magnetic moments grow $\sim f_\mu$ along the renormalization-group flow, one might naively expect that the mean magnetic moment to be decimated, $\overline{\mu}_0$, also grows $\sim f_\mu$. This would imply that the above probability becomes negative (notice $\rho_{\beta,0}$ is nonzero). Therefore, correlations between the fields and moments ensure that this probability remains well defined.

By Laplace transforming (A11), we finally arrive at

$$\frac{\partial\hat{\rho}}{\partial\Gamma} = \alpha b\frac{\partial\hat{\rho}}{\partial m} + \pi_0(\hat{\rho}^2-\hat{\rho}), \tag{A12}$$

where $\hat{\rho}(b,m) = \int e^{-b\beta}\rho'(\beta,m)d\beta$ and $\rho'(\beta,m) = \int e^{-m\mu}\rho(\beta,\mu)d\mu$. [The term $\alpha\partial\rho'(0,m)/\partial m$ also vanishes because of the correlations between fields and magnetic moments.] The first term on the right-hand side of Eq. (A12) is the desired leading correction to the fixed-point flow equation (A7). Inspection of Eq. (A12), guided by the fixed-point result (A8), yields

$$\hat{\rho}^*(b,m;\Gamma) = \left[1+F\left(\Gamma+\frac{m}{\alpha b},b\right)\exp\left(-\pi_0\frac{m}{\alpha b}\right)\right]^{-1},$$

where $F(y,b)$ is an integration constant which depends on b and on the combination $y = \Gamma + \frac{m}{\alpha b}$, which implies $m/b \propto \Gamma$, i.e., $f_\beta/f_\mu \propto \Gamma$. To see this clearly, let us compute F from some initial conditions.

Consider first a perfectly correlated one, i.e.,

$$\hat{\rho}(b,m;0) \equiv \hat{\rho}_{\rm corr} = \left(1+\frac{b}{\rho_{\beta0}}+\frac{m}{\rho_{\mu0}}\right)^{-1}. \tag{A13}$$

In this case, $F(y,b) = b(1+\alpha\rho_{\beta0}y/\rho_{\mu0})e^{\pi_0 y}/\rho_{\beta0}$. Thus, $\hat{\rho}^*(b,m;\Gamma) = \hat{\rho}(b,m;\Gamma\to\infty)$ with

$$\hat{\rho}^*(b,m;\Gamma) = \left(1+\frac{\alpha f_\beta b + f_\mu m}{\rho_{\mu0}}\right)^{-1}, \tag{A14}$$

with $f_\mu = e^{\pi_0\Gamma}$ as expected, and $f_\beta = \Gamma e^{\pi_0\Gamma}[1+\mathcal{O}(\alpha\Gamma)^{-1}]$. Notice that $\hat{\rho}^*$ is of the perfectly correlated type (A9). Finally, we obtain the scale factor $f_\beta \sim \Gamma f_\mu$, which satisfies the requirements that $f_\mu/f_\beta \to 0$ and $\dot{f}_\mu/f_\mu = \dot{f}_\beta/f_\beta = \mathcal{P}_0 = \pi_0$ in the limit $\Gamma\to\infty$.

To convince ourselves that $\hat{\rho}^*$ is the relevant attractive fixed-point distribution, consider, for example, an initial condition that is totally at odds with Eq. (A13): the perfectly uncorrelated case

$$\hat{\rho}(b,m;0) \equiv \hat{\rho}_{\rm uncorr} = \left(1+\frac{b}{\rho_{\beta0}}\right)^{-1}\left(1+\frac{m}{\rho_{\mu0}}\right)^{-1}.$$

In this case, $F(y,b) = b[1+\alpha y(\rho_{\beta0}+b)/\rho_{\mu0}]e^{\pi_0 y}/\rho_{\beta0}$, which yields

$$\hat{\rho}(b,m;\Gamma) = \left[1+\frac{\alpha f_\beta b + f_\mu m}{\rho_{\mu0}} + \mathcal{O}\left(b,\frac{1}{\Gamma}\right)\right]^{-1}.$$

In the limit $\Gamma\to\infty$, and $b,m\to0$, this distribution flows to the attractive solution $\hat{\rho}^*(b,m;\Gamma)$ (A14). Since both uncorrelated and perfectly correlated initial conditions flow to the same (correlated) fixed-point solution (A14), we expect all well-behaved (ferromagnetic) initial distributions to flow toward this fixed point. We have also checked this numerically in Ref. 26. After the inverse Laplace transformation, we finally obtain

$$\rho^*(\beta,\mu;\Gamma) = \rho_{\beta0}\rho_{\mu0}e^{-\rho_{\beta0}\beta}\delta(\rho_{\beta0}\beta-\rho_{\mu0}\mu), \tag{A15}$$

with $\rho_{\mu0} = \rho_0/f_\mu$ and $\rho_{\beta0} = \rho_0/(\alpha f_\beta)$.

[1] N. Goldenfeld, *Lectures on Phase Transitions and the Renormalization Group* (Addison-Wesley, Reading, 1992).
[2] M. E. Fisher, Rev. Mod. Phys. **70**, 653 (1998).
[3] A. B. Harris, J. Phys. C: Solid State Phys. **7**, 1671 (1974).
[4] R. B. Griffiths, Phys. Rev. Lett. **23**, 17 (1969).
[5] B. M. McCoy, Phys. Rev. Lett. **23**, 383 (1969).
[6] Y. Imry, Phys. Rev. B **15**, 4448 (1977).
[7] M. J. Thill and D. A. Huse, Phys. A (Amsterdam) **214**, 321 (1995).
[8] M. Guo, R. N. Bhatt, and D. A. Huse, Phys. Rev. B **54**, 3336 (1996).
[9] A. P. Young and H. Rieger, Phys. Rev. B **53**, 8486 (1996).
[10] D. S. Fisher, Phys. Rev. Lett. **69**, 534 (1992).
[11] D. S. Fisher, Phys. Rev. B **51**, 6411 (1995).
[12] A. J. Leggett, S. Chakravarty, A. T. Dorsey, M. P. A. Fisher, A. Garg, and W. Zwerger, Rev. Mod. Phys. **59**, 1 (1987).
[13] A. J. Millis, D. K. Morr, and J. Schmalian, Phys. Rev. Lett. **87**, 167202 (2001).
[14] A. J. Millis, D. K. Morr, and J. Schmalian, Phys. Rev. B **66**, 174433 (2002).
[15] T. Vojta, Phys. Rev. Lett. **90**, 107202 (2003).
[16] G. Schehr and H. Rieger, Phys. Rev. Lett. **96**, 227201 (2006).
[17] G. Schehr and H. Rieger, J. Stat. Mech. **4**, P04012 (2008).
[18] J. A. Hoyos and T. Vojta, Phys. Rev. Lett. **100**, 240601 (2008).
[19] A. O. Caldeira and A. J. Leggett, Phys. Rev. Lett. **46**, 211 (1981).
[20] S.-k. Ma, C. Dasgupta, and C.-k. Hu, Phys. Rev. Lett. **43**, 1434 (1979).
[21] C. Dasgupta and S.-k. Ma, Phys. Rev. B **22**, 1305 (1980).
[22] F. Iglói and C. Monthus, Phys. Rep. **412**, 277 (2005).
[23] F. Iglói, Phys. Rev. B **65**, 064416 (2002).
[24] If $\dot{f}_\zeta/f_\zeta$ vanishes more slowly than $1/f_\zeta$, then the first term on the right-hand side of Eq. (27) is the leading one yielding $\mathcal{P}^* = \eta^{-1}$, which is not normalizable. If, in turn, $1/f_\zeta$ vanishes more slowly, then the second and third terms on the right-hand side of Eq. (27) become the leading ones. After a Laplace transformation, one finds that $\mathcal{P}^* = J_1(2P_0\eta)/(2\eta)$, with J_1 being the Bessel function of first kind, which has nonphysical negative values.
[25] J. A. Hoyos (unpublished).

[26]T. Vojta and J. A. Hoyos, Phys. E (Amsterdam) **42**, 383 (2010).
[27]S. K. Kehrein and A. Mielke, Phys. Lett. A **219**, 313 (1996).
[28]R. Bulla, N.-H. Tong, and M. Vojta, Phys. Rev. Lett. **91**, 170601 (2003).
[29]T. Vojta, J. Phys. A: Math. Gen. **36**, 10921 (2003).
[30]F. Hrahsheh, D. Nozadze, and T. Vojta, Phys. Rev. B **83**, 224402 (2011).
[31]C. Svoboda, D. Nozadze, F. Hrahsheh, and T. Vojta, Europhys. Lett. **97**, 20007 (2012).
[32]P. Werner, K. Völker, M. Troyer, and S. Chakravarty, Phys. Rev. Lett. **94**, 047201 (2005).
[33]T. R. Kirkpatrick and D. Belitz, Phys. Rev. Lett. **76**, 2571 (1996).
[34]R. Narayanan, T. Vojta, D. Belitz, and T. R. Kirkpatrick, Phys. Rev. Lett. **82**, 5132 (1999).
[35]R. Narayanan, T. Vojta, D. Belitz, and T. R. Kirkpatrick, Phys. Rev. B **60**, 10150 (1999).
[36]O. Motrunich, S.-C. Mau, D. A. Huse, and D. S. Fisher, Phys. Rev. B **61**, 1160 (2000).
[37]I. A. Kovács and F. Iglói, Phys. Rev. B **83**, 174207 (2011).
[38]T. Senthil and S. Sachdev, Phys. Rev. Lett. **77**, 5292 (1996).
[39]J. A. Hoyos and T. Vojta, Phys. Rev. B **74**, 140401 (2006).
[40]J. A. Hertz, Phys. Rev. B **14**, 1165 (1976).
[41]G. R. Stewart, Rev. Mod. Phys. **73**, 797 (2001).
[42]G. R. Stewart, Rev. Mod. Phys. **78**, 743 (2006).
[43]H. v. Löhneysen, A. Rosch, M. Vojta, and P. Wölfle, Rev. Mod. Phys. **79**, 1015 (2007).
[44]A. H. Castro Neto and B. A. Jones, Phys. Rev. B **62**, 14975 (2000).
[45]S. Guo, D. P. Young, R. T. Macaluso, D. A. Browne, N. L. Henderson, J. Y. Chan, L. L. Henry, and J. F. DiTusa, Phys. Rev. Lett. **100**, 017209 (2008).
[46]T. Westerkamp, M. Deppe, R. Küchler, M. Brando, C. Geibel, P. Gegenwart, A. P. Pikul, and F. Steglich, Phys. Rev. Lett. **102**, 206404 (2009).
[47]S. Ubaid-Kassis, T. Vojta, and A. Schroeder, Phys. Rev. Lett. **104**, 066402 (2010).
[48]T. Vojta, J. Phys. A: Math. Gen. **39**, R143 (2006).
[49]T. Vojta, J. Low Temp. Phys. **161**, 299 (2010).
[50]T. Vojta and J. Schmalian, Phys. Rev. B **72**, 045438 (2005).
[51]J. A. Hoyos, C. Kotabage, and T. Vojta, Phys. Rev. Lett. **99**, 230601 (2007).
[52]T. Vojta, C. Kotabage, and J. A. Hoyos, Phys. Rev. B **79**, 024401 (2009).
[53]T. Vojta, J. A. Hoyos, P. Mohan, and R. Narayanan, J. Phys.: Condens. Matter **23**, 094206 (2011).
[54]E. Altman, Y. Kafri, A. Polkovnikov, and G. Refael, Phys. Rev. Lett. **93**, 150402 (2004).
[55]S. Sachdev, *Quantum Phase Transitions* (Cambridge University Press, Cambridge, UK, 1999).